# Environmental chemical sensing using small drones: A review

Javier Burgués, Santiago Marco

a. Institute for Bioengineering of Catalonia (IBEC), The Barcelona Institute of Science and Technology, Baldiri Reixac 10-12, 08028 Barcelona, Spain
b. Department of Electronics and Biomedical Engineering, Universitat de Barcelona, Marti i Franqués 1, 08028 Barcelona, Spain

**Abstract**

Recent advances in miniaturization of chemical instrumentation and in low-cost small drones are catalyzing exponential growth in the use of such platforms for environmental chemical sensing applications. The versatility of chemically sensitive drones is reflected by their rapid adoption in scientific, industrial, and regulatory domains, such as in atmospheric research studies, industrial emission monitoring, and in enforcement of environmental regulations. As a result of this interdisciplinarity, progress to date has been reported across a broad spread of scientific and non-scientific databases, including scientific journals, press releases, company websites, and field reports. The aim of this paper is to assemble all of these pieces of information into a comprehensive, structured and updated review of the field of chemical sensing using small drones. We exhaustively review current and emerging applications of this technology, as well as sensing platforms and algorithms developed by research groups and companies for tasks such as gas concentration mapping, source localization, and flux estimation. We conclude with a discussion of the most pressing technological and regulatory limitations in current practice, and how these could be addressed by future research.

**Keywords**

Unmanned aircraft systems; Remotely piloted aircraft systems; Chemical sensors; Gas sensors; Environmental monitoring; Industrial emission monitoring

## 1. Introduction

Small drones equipped with chemical sensing payloads are emerging as a valuable tool in different metrology disciplines such as atmospheric chemistry, industrial emission monitoring, environmental law enforcement, and precision agriculture. Here we define a small drone as a remotely piloted aircraft system (RPAS) or unmanned aircraft system (UAS) with a maximum take-off weight (MTOW) of <25 kg, i.e. the weight of the drone including the batteries (or fuel) and the payload (Hugenholtz et al., 2012). Having an MTOW of <25 kg represents an important regulatory advantage, as they can be operated in many countries without the need for a flight permit from the aviation authorities (under certain operational conditions). A chemical sensing payload gives drones a unique set of abilities, such as producing 3D air quality maps with high spatial resolution, monitoring toxic gases in dangerous or hard-to-reach locations (e.g. chimneys, volcanoes, etc.), or analyzing the chemical composition of the lower atmosphere. In recent years, there has been an upward trend in the number of published scientific papers on the use of small drones for chemical sensing applications (Fig. 1). We believe that this increase is due to growth in the commercial drone manufacturing sector, which now offers a broad selection of small drones that are affordable for most research groups, the availability of low-cost, lightweight chemical sensing instruments, as well as increasing social concern and tightening regulations on air pollution and global warming. The growing interest in drones for gas sensing applications is also evident from the recent market appearance of gas detectors specifically designed for drone applications and drones with integrated gas sensors.

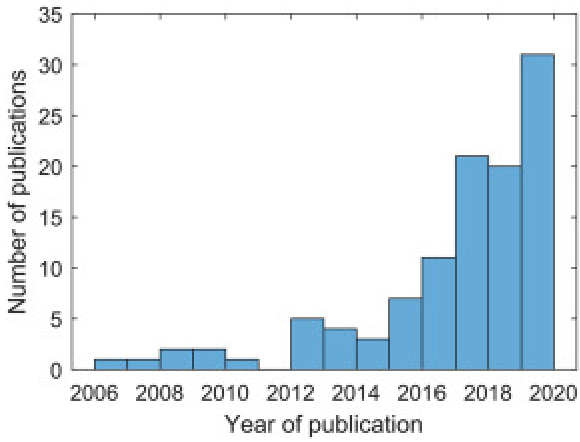


Fig. 1. Published papers per year in the field of small drones for chemical sensing applications. The data were compiled by searching for titles, abstracts, or keywords of journal articles, reviews and conference proceedings that contained some of the keywords listed in Table S1 (Supplementary material), in Google Scholar, Web of Science and Scopus databases.

Increasing regulatory pressure to monitor and control industrial greenhouse gas (GHG) emissions and air pollutants has forced industry operators to search for cost-effective methods to regularly monitor their emissions (Brinkmann et al., 2018). The oil and gas (O&G) industry is beginning to realize the potential benefits of integrating drone technology into their operations (TOTAL Group, 2019), and several drone manufacturers have developed drones equipped with methane sensors to serve the O&G sector. Similarly, in the waste management industry, operators of solid waste landfills (SWLs) and wastewater management plants (WWTPs) are already experimenting with drones equipped with gas detectors as a way to reduce the costs and risks of walkover surveys using hand-held detectors (Emran et al., 2017). Environmental agencies and police departments in some countries currently use drones to check for compliance with air emission regulations. For example, the Maritime Authorities in Denmark, Hong Kong, and other countries use drones to detect ships breaking international rules governing the maximum sulfur content of marine fuel (Zhou et al., 2019). In Poland, the police departments of some cities have started using drones to 'sniff' the exhaust plumes of chimneys in residential neighborhoods to find polluters using low-quality fuel for domestic heating (Scentroid, 2018).

Small drones are useful for atmospheric chemistry research because they can densely sample regions of the atmosphere that were previously difficult to access with existing methodologies, such as satellite observations, manned aircraft, or weather balloons (Villa et al., 2016). They have been widely used to investigate the concentration of GHGs and other air pollutants in the lower atmosphere (0–2000 m), to analyze the composition of volcanic plumes, and to quantify GHG emissions from wildfires or permafrost. In agriculture, data on gases such as CH4 and CO2 can be useful for indicating crop health or monitoring emissions from livestock that may be spread over large areas.

Drones are also an excellent platform for roboticists to develop and test algorithms for gas source localization (GSL) and gas concentration mapping (GCM). The use of mobile robots for GSL and GCM has been a focus of research since the 1990s, and remains an open problem even today, partly due to the limited locomotion capabilities of terrestrial robots (Hernandez Bennetts et al., 2012a). The 3D sampling capabilities of drones creates new possibilities in this field, for example implementing bioinspired algorithms based on the 3D searching behavior of some flying insects, such as the moth, which efficiently navigate odor plumes for mating and foraging (Rahbar et al., 2017).

The rapid increase in the use of gas-sensitive drones across these many disciplines has generated a vast amount of information (platforms, sensors, algorithms, results, etc.) spread across scientific and non-scientific databases such as scientific journals, conference proceedings, websites, blogs, press releases, technical reports, and field reports. Even if we consider only scientific publications, relevant papers have been published under >20 journal classifications, including: sensors, unmanned aerial vehicles, remote sensing, atmospheric research, applied sciences, waste management, ecology, optics, applied physics, geophysics, meteorology, environmental technology, robotics, instrumentation, dynamic systems and control, consumer electronics and neuroengineering. Having such diverse information sources is problematic because the parties involved in developing and using gas-sensitive drones (e.g. researchers, industry, environmental agencies, etc.) are often unaware of the state of the art in the field.

The aim of this paper is to assemble all of this information, in order to provide a comprehensive and updated review of the field of chemical sensing using small drones. Section 2 summarizes previous literature reviews on this topic and highlights the need for a comprehensive review. Section 3 reviews the drones and chemical instrumentation payloads that have been developed for gas sensing applications, appraises advantages and disadvantages of these payloads, and highlights important considerations regarding their installation on the drone. Section 4 explains the main algorithms developed to address four transversal gas sensing tasks (concentration mapping, source localization, source identification, and flux quantification). Section 5 overviews current and emergent applications for gas-sensing drones. The paper concludes with a discussion of the most pressing technological and regulatory limitations in current practice, and how these could be addressed by future research.

## 2. Previous literature reviews

The most comprehensive review of this field was presented by Villa et al. (2016), who covered the use of small drones for meteorology (i.e. wind, temperature, humidity) and chemical sensing in the lower atmosphere. This review was published just before the “boom” of scientific papers on this topic in 2017 (c.f. Fig. 1), so obviously it does not include many important applications and technologies. Two minor reviews were presented by Pajares (2015) and Schuyler and Guzman (2017). The first review, which is focused on the field of remote sensing, dedicates a small section to the use of drones for air quality measurement and volcanic plume monitoring. The second review covers several reports on monitoring atmospheric trace gases with small drones. None of these reviews covered the different algorithms that have been developed over time for gas-sensing tasks such as GSL or GCM. They also did not review the numerous drone platforms and sensing systems that have been commercialized in the last years.

## 3. Drones and chemical instrumentation payloads

### 3.1. Small drones

A small drone, often termed microdrone or small UAS (sUAS), resembles a conventional radio-controlled (RC) hobby aircraft but can carry small payloads (typically <4–5 kg), and has an integrated flight control system that enables semi- or fully autonomous flight. The two main types of drones are fixed-wing (FW) and rotary-wing (RW) platforms. FW aircraft are aerodynamically efficient, enabling them to fly at high speeds for a long time, thus covering long distances in a single flight. This makes them convenient for screening large areas, such as in detecting pipeline leaks. However, small FW drones have practical limitations related to their low payload capacity and need for a catapult launch system or a runway for take-off and landing. Also, they must continuously remain in relatively fast forward motion, which limits the spatial resolution of the acquired measurements. The spatial resolution of a mobile measurement is the product of the vehicle's speed and the instrument response time. They are also unsuitable for applications that require stationary measurements, such as when monitoring chimney exhaust gases, or that require low-height or slow-speed flights, such as when surveying indoor spaces, urban areas, or industrial plants.

RW drones, or rotorcrafts, can overcome some of these limitations, because of their capacity for vertical take-off and landing (VTOL), autonomous hovering based on Global Positioning System (GPS), slow cruise speed, high maneuverability, and higher payload. RW platforms can be classified according to the number of rotors as helicopters (1 rotor), quadrotors (4 rotors), hexarotors (6 rotors) and octorotors (8 rotors). Small-scale (i.e. <10 kg) rotorcraft with 4–6 rotors are generally preferred due to their mechanical simplicity, which translates into lower costs, greater reliability and easier maintenance. For example, the DJI Matrice 600 hexarotor (~9 kg with batteries) is currently a highly popular drone due to its high payload capacity of 6 kg, flight time of ~30 min (without payload), and moderate price of ~$6000. A RW drone can be flown very close to gas-emitting structures such as chimneys, tanks, or flares, allowing close-range measurements that are not feasible with FW platforms. However, due to their lower speed and flight range (a fully loaded DJI Matrice 600 can only fly for 15 min) surveying large areas requires multiple flights, increasing mission time and operational costs.

The biggest shortcoming of RW platforms for chemical sensing is the strong vertical airflow generated by its rotors (the so-called downwash, Fig. 2). The downwash disturbs the local air distribution around the drone (especially below it) and can have negative consequences for the utility of the on-board sensor data. The aerodynamic characteristics of the downwash generated by rotorcrafts have been simulated using Computer Fluid Dynamics technology (CFD) (Eu et al., 2014; Eu and Yap, 2018; Koziar et al., 2019; Kuantama et al., 2019; Luo et al., 2016; McKinney et al., 2019; Roldán et al., 2015; Sanchez-Cuevas et al., 2017), experimentally measured with anemometers (Prudden et al., 2016; Sjöholm et al., 2014; Wolf et al., 2017), or particle tracking velocimetry (PTV) systems (Shigaki et al., 2018; Shukla and Komerath, 2018), and visualized using smoke experiments (Hollenbeck et al., 2019b; Hutchinson et al., 2019; Kang et al., 2018; Luo et al., 2017; Neumann et al., 2012; Prudden et al., 2016; Smith et al., 2016). While airflow is typically negligible at 40–50 cm above the drone (Alvarado et al., 2017; Palomaki et al., 2017) and at horizontal distances of >70–80 cm (Prudden et al., 2016; Wolf et al., 2017), the downwash can extend several meters below the propellers even for lightweight drones of 5 kg (Greatwood et al., 2017). The worst effects of the local mixing produced by the rotors occur when measuring across strong spatial gradients, such as in chemical plumes (Hutchinson et al., 2019; Neumann et al., 2012).

Fig. 2. Downwash of a hovering DJI Matrice 600 drone visualized using colored smoke (Crazzolara et al., 2019).

### 3.2. Chemical instrumentation

The limited payload capacity on small drones requires lightweight, low-power instrumentation. Five types of chemical sensing instruments can be mounted on a small drone: low-cost sensors, multi-sensor systems, electronic noses, high-precision optical analyzers, and optical gas imaging cameras.

### 3.2.1. Low-cost chemical sensors

Low-cost (<$300) chemical sensors are miniaturized devices (Fig. 3) that provide a real-time output reflecting the concentration of gases and volatile organic compounds (VOCs) in contact with the sensor. The minimal size, low weight, low power requirements, and simplicity of the conditioning electronics makes it straightforward to integrate them into fixed and portable measurement systems, such as those commonly used for industrial safety (Rezende et al., 2019), environmental monitoring (Baron and Saffell, 2017; Fine et al., 2010), automotive (Tuller, 2013; Wales et al., 2015), food analysis (Loutfi et al., 2015), and biomedicine applications (Vincent and Gardner, 2016). For example, chemical sensors are the basis of domestic and industrial carbon monoxide alarms (Stetter and Pan, 1994), personal exposure monitors (portable devices that alert workers when they are being exposed to poisonous gases and VOCs) (Piedrahita et al., 2014), breathalyzers (devices for estimating blood alcohol content (BAC) from a breath sample) (Zuliani et al., 2020), capnography monitors (devices for measuring time-resolved CO2 concentration in exhaled breath during anesthesia) (Yang et al., 2015), indoor and outdoor air quality units (Burgués et al., 2020; Tran et al., 2017), and electronic noses (devices to quantify odor intensity and classify odor types) (Gardner and Bartlett, 1999). Low-cost sensors are also used to monitor CO2 levels in HVAC (Heating, ventilation, and air conditioning) units (Nassif, 2012), and NOx emissions in the exhaust systems of many automobiles (Tuller, 2013).


Fig. 3. Examples of low-cost chemical sensors. (From left to right) MOX sensor (Model: Figaro TGS 8100); AGS sensor (Model: Alphasense CO-AF); PID (Model: RAE Systems PID 10.6 eV); (d) NDIR sensor (Model: CozIR by Gas Sensing Solutions).

Among the various low-cost gas-sensing technologies (see a review by Gründler (2007)), the most popular ones for drone applications are amperometric gas sensors (AGS), metal oxide semiconductor (MOX or MOS) sensors, non-dispersive infrared (NDIR) sensors, and photo-ionization detectors (PIDs). Several text books review the working principles, advantages, limitations, and applications of each technology (Gründler, 2007; Seiyama, 2013), so we will provide only a brief summary of each technology here.

Amperometric gas sensors (AGS), i.e. electrochemical gas sensors based on amperometry, are one of the most promising sensor technologies for measuring inorganic gases at parts-per-billion (ppb) and parts-per-million (ppm) concentrations. These sensors are often termed electrochemical sensors, but we prefer the terminology AGS to distinguish them from other electrochemical sensors, such as conductometric and potentiometric sensors (Stetter and Li, 2008). The most common target gases that an AGS can detect are O2, CO, SO2, NO, NO2, O3,

$NH_3$, and $H_2S$. These sensors are based on the electrochemical reactions that take place in an electrochemical cell, typically consisting of three electrodes (working, counter and reference) immersed in a liquid electrolyte solution (a mineral acid or organic solvent with an added salt) containing a catalyst. Initially, the gas diffuses into the sensor through a gas-porous membrane which limits the supply of gas to the sensor to ensure diffusion-limited reactions, and can also filter out some chemical interferences. Under diffusion-limited reaction conditions, the flow of current between the working and counter electrodes (output signal of the sensor) is linearly correlated with the concentration of the target gas, and the output signal is less sensitive to the temperature of the reaction than when the gas supply is not limited. A potentiostat maintains the working electrode at a fixed potential with respect to the reference electrode to ensure complete reaction of the target gas. Selectivity is achieved by the choice of catalyst, by optimizing the working electrode material, and by using chemical filters to remove key interfering substances. Another way of improving the selectivity is to combine the output of multiple AGS using multivariate regression models (Spinelle et al., 2017, Spinelle et al., 2015); a classical example is the use of an $O_3$ sensor to compensate the known cross-sensitivity of $NO_2$ sensors to this gas, and vice versa (Baron and Saffell, 2017).

In addition to providing linear measurements, and being cheap, reliable, and quite selective for some gases, AGS also have negligible power consumption (<1 mW), making them ideal sensors for battery-operated instruments. Their main problems are the slow response and recovery times (30–60 s), high cross-sensitivity to ambient temperature, drift of their parameters with time, and their limited lifetime (time until 80% of original signal) of ~2 years due to consumption or evaporation of the liquid electrolyte (Hunter et al., 2020). The latest AGS sensors developed by Figaro Engineering Inc. (Japan) for carbon monoxide (e.g. model TGS 5141) guarantee an exceptionally long lifespan of 10 years by using a proprietary electrolyte solution that does not require a water reservoir. Recent co-location field studies have found that hourly-averaged measurements of criteria pollutants ($O_3$, CO, $SO_2$, NO and $NO_2$) recorded by several commercial instruments based on AGS showed good agreement with similar measurements made by approved reference analyzers (Borrego et al., 2018, Borrego et al., 2016; Chatzidiakou et al., 2019; Collier-Oxandale et al., 2020; Jiao et al., 2016), provided that the user corrects for baseline drift of the AGS due to variation in ambient temperature and humidity (Wei et al., 2018). The agreement with reference instruments can be often improved by using multivariate predictive models that take into account the signals of multiple AGS sensors and temperature and humidity readings (Spinelle et al., 2017, Spinelle et al., 2015).

Metal oxide semiconductor (MOX or MOS) sensors, also termed semiconductor sensors or chemoresistors, are a conductometric type of electrochemical sensor. They are mostly used for measuring VOCs, at the ppm and sub-ppm level, but can also be used as an alternative technology for measuring some of the gases accessible to AGS (e.g. carbon monoxide) (Burgués et al., 2018). The working principle is based on the fact that certain semiconducting metal oxides (e.g. tin dioxide, $SnO_2$) change their electrical resistance upon exposure to gases at high working temperatures (typically 150–500 °C). The sensing material is deposited over a substrate with integrated electrodes (for readout of the electrical resistance) and a heater resistor (to heat up the sensing material). Although MOX sensors are inherently non-specific, their selectivity can be somewhat improved by a number of techniques, the most popular of which are using multivariate predictive models that take into account the response across a sensor array (Marco and Gutierrez-Galvez, 2012), exploiting the dynamic response due to a sampling transient or temperature modulation (Gutierrez-Osuna et al., 2003; Lee and Reedy, 1999), doping the metal oxide layer with noble metals (Korotcenkov and Cho, 2017), or using chemical filters (Kitsukawa et al., 2000; Korotcenkov and Cho, 2013). Methods for improving the sensor sensitivity and selectivity are exhaustively reviewed by Korotcenkov and Cho (2013) and Wang et al. (2010).

MOX sensors are smaller, faster (response time of 10–20 s), and more durable (a lifetime of >10 years is typical) than AGS, although the latter are more selective and power efficient. The output signal of a MOX sensor is highly susceptible to humidity changes (indeed some metal oxides are used to fabricate humidity sensors (Chen and Lu, 2005)), although this can be effectively remedied by modulating its working temperature (Burgués and Marco, 2018a). Thanks to microelectromechanical systems (MEMS) technology, MOX sensors can now be fabricated with a miniaturized sensing layer deposited over a micro-hotplate, enabling sensors with a footprint of a few mm2, a response time of 5–10 s, and power rating of 15–30 mW. The response time and power consumption can be further reduced by signal processing techniques (Burgués et al., 2019b; Monroy et al., 2012) and duty cycling operation (Burgués and Marco, 2018b).

Non-dispersive infrared (NDIR) sensors are miniaturized optical analyzers composed of a broadband infrared (IR) lamp, a sample chamber, a narrowband optical filter, and an IR detector. The working principle is based on the optical absorption of some gases when they are excited with IR light. The difference between the amount of light emitted by the lamp and the light received by the detector is proportional to the concentration of the target gas in the sample chamber. The role of the optical filter is to filter out all wavelengths except those corresponding to the absorption band of the target gas. Since the measurement is based on a physical property of the gas instead of physicochemical reactions, sensors based on optical absorption avoid some shortcomings of electrochemical sensors, such as poisoning by silicone vapors, and inter-device variability. NDIR technology is particularly well-suited for measuring CO2 because it has a strong and non-overlapping absorption peak at 4.26 mm in the mid-IR region, which enables devices with short path lengths (1–2 cm). Although NDIR sensors are also commercially available for CH4, they have limited practical use due to the lower absorption coefficient and high cross-sensitivity to other hydrocarbons.

Low-cost NDIR sensors have limited accuracy because of the influence of ambient temperature and pressure on light absorption (Martin et al., 2017). For example, the accuracy of a low-cost CO2 sensor is approximately 30 ppm + 3% of the reading (Dinh et al., 2016). With appropriate temperature and pressure control, the accuracy can be improved to 1% of the reading (see Section 3.2.3). NDIR sensors are more expensive and power hungry than other low-cost technologies, although new IR light-emitting diode (LED) light sources have been developed that allow NDIR sensors to operate at much lower power (3 mW) than before (50 to 200 mW) (Hodgkinson and Tatam, 2013).

Photoionization detectors (PIDs) are broad-band sensors that can detect a wide range of VOCs and some inorganic gases. They consist of an UV lamp shining on a small cell containing the gas sample. The UV light (typically 10.6 eV) ionizes the VOCs in the sample, resulting in electrons and positive ions being ejected towards various electrodes placed inside the chamber, producing a current proportional to the gas concentration. Typically, PIDs can measure concentrations of 10 ppb to 10,000 ppm, although they are most accurate in the lower end of the range (up to about 2000 ppm) where the gas concentration is linearly correlated with the sensor signal (RAE-Systems, 2014). The response time of PID instruments (typically a few seconds) is usually determined by the rate at which the sample is pumped through and then flushed completely from the detection chamber. Some miniaturized designs, such as the miniPID 200A by Aurora Scientific (Canada), can achieve extraordinarily low response times of few milliseconds. Hand-held instruments based on PIDs are commonly used in industrial sites and military applications for monitoring toxic VOCs (Licen et al., 2020). The main problems of this type of instrument are the relatively high cost, the low specificity, and their inability to detect compounds with high ionization energy (e.g. noble gases, CO, $CO_2$, $SO_2$, $O_3$).

### 3.2.2. Multi-sensor systems

Most environmental applications need to monitor more than one gas simultaneously, so a single chemical sensor is not sufficient. Multi-sensor systems incorporate several chemical sensors into one instrument, and also include the necessary electronics, data logging, fluidics components, and power management systems (Fig. 4). There are two types of systems: standalone and integrated. Standalone systems include their own GPS, battery, and radio link, allowing them to operate autonomously. Integrated systems obtain these resources from the drone, and are those lightweight systems that can only be used with specific drone models. Table S1 (Supplementary material) lists some commercial examples of both types of systems. Most multi-sensor systems are lightweight (<2 kg) and can typically host 5 to 10 sensors (mostly AGS but also PIDs, NDIR, and less frequently MOX sensors). The sensors are typically housed in a sensing chamber where ambient air is introduced by a pump, or in some cases a fan. Some systems allow the user to configure the sensor suite, while others have a sensor suite tailored for a specific application (e.g. ship emission monitoring, volcanic research, etc.). Some research groups have also developed their own multi-sensor systems with customized sensor suites (Carrozzo et al., 2018; Zhou et al., 2017).

Fig. 4. Commercial multi-sensor unit Sniffer 4D equipped with 5 AGS sensors, 1 PID and 1 NDIR sensor. Copyright Soarability Technologies. Used with permission.

### 3.2.3. Electronic nose

An electronic nose (e-nose) or sensor array is a software-hardware system that uses a combination of multiple partially selective sensors and pattern recognition algorithms to selectively quantify or discriminate gases and odors (Gardner and Bartlett, 1999). Some applications of e-noses include medical diagnostics (Wojnowski et al., 2019), food quality control (Loutfi et al., 2015), aroma classification (Kiani et al., 2016), and industrial odor measurements (Bax et al., 2020). Odor recognition and intensity estimation (as human beings perceive it) is particularly difficult to achieve with selective optical analyzers that respond only to one compound. E-noses overcome this difficulty by analyzing the multivariate response pattern of a diverse and redundant array of broadband sensors sensitive to a wide array of VOCs and gases (in some sense inspired by the mammalian olfactory system). The sensor array can be heterogeneous (i.e. contain different sensor technologies) or homogeneous (i.e. all sensors are of the same technology). In the latter case, the sensor units are selected from different models or manufacturers, or are operated in a different manner, for example by changing the working temperature of MOX sensors. Linear predictive models such as partial least squares (PLS), or non-linear methods based on support vector regression (SVM) or artificial neural networks (ANN) are commonly used to predict odor intensity (Marco and Gutierrez-Galvez, 2012).

One main problem of e-noses is that they are subject to the same limitations as the low-cost sensors from which they are made. If any of the sensors drift, the e-nose output will drift as well, and correcting the drift of a sensor array is more challenging than in a single sensor (Romain and Nicolas, 2010). Periodic recalibration of the electronic nose is required to maintain its accuracy over time (Zhang and Zhang, 2014). To reduce recalibration effort, calibration transfer methodologies have been proposed in the literature (Fonollosa et al., 2016). Sensor chambers, which are necessary to accommodate all sensors (10–15 sensors are typical), increase the system's response time. Power consumption may be also an issue if, for example, the e-nose is based on isothermally-operated MOX sensors. Because of these issues and to maximize accuracy, e-noses are typically operated in highly controlled laboratory conditions with long measurement cycles consisting of air-gas-air exposures. Recent attempts have been made to use portable e-noses with miniaturized sensing chambers mounted on drones (DAM-IBEC, 2019). For this application, it is critical to design customized small chambers that would enable fast measurements (Burgués et al., 2019b). Systems where sensors are directly exposed to air can be faster, but then the measurement point is directly located on the drone body, which could be a suboptimal location for some applications (for instance, to measure near diffusive area sources of pollution). More details on the installation of e-noses in drones are provided in Section 3.3.

### 3.2.4. High-precision optical analyzers

Optical gas analyzers exploit the characteristic absorption spectra of some gases when they are excited with IR or UV light. They can selectively detect, at the ppb level, compounds with non-overlapping spectral regions, such as CO2 or CH4 in the mid-IR and O3 in the near-UV (Andersen et al., 2010; Popa et al., 2019). Since optical analyzers measure a physical property of the gas, in principle these measurements can be faster and more reliable than those based on an active sensitive layer involving physicochemical reactions (e.g. AGS, MOX). To increase the quality of the measurements, high-precision optical instruments include sophisticated components such as lasers, high reflectivity mirrors, quartz coated cavities, and temperature and pressure compensation systems, which results in bulky, heavy, power hungry, and expensive instruments. For example, the LI-850 CO2 NDIR analyzer (LI-COR Inc., Lincoln, NE, USA) uses a thermostatically controlled optical path and automatic pressure compensation (Fig. 5) to provide a limit of detection (LOD) of 1.5 ppm and accuracy of 1.5% of the reading (compared to 30 ppm ± 3% for low-cost NDIRs). The LI-850 weighs 1.3 kg, consumes 5 W of power, and requires 12–30 V DC. In contrast, a low-cost NDIR sensor weights a few grams, consumes a few mW of power, and requires <5 V.

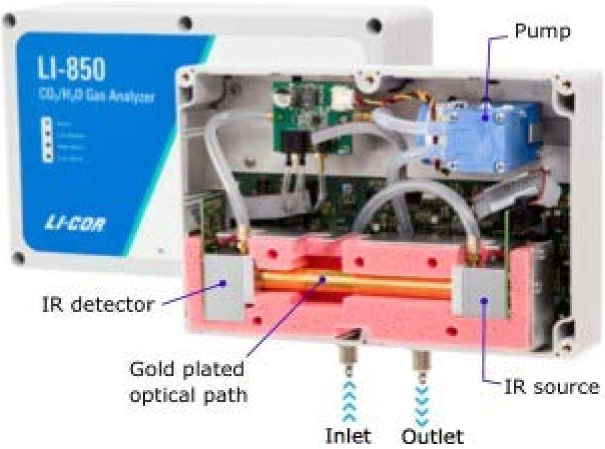


Fig. 5. Interior of a closed-path LI-850 NDIR CO2 analyzer. Copyright LI-COR Inc. Used with permission.

Laser-based techniques (Tittel et al., 2008), also known as laser absorption spectroscopy (LAS), achieve selectivity for a target gas, typically methane (Wang et al., 2019), without the need for narrowband filters (as in NDIR). The most common LAS technique, known as TDLAS, employs a tunable diode laser (TDL) modulated in frequency as a light source. The laser beam can operate in flow-through (closed-path) cells or via open atmospheric paths. Closed-path designs (CP-TDL) achieve better quality measurements by using multi-pass cells with temperature and pressure compensation, although the time required to fill the gas cell results in a slower response time. Open-path instruments (OP-TDL) are generally less accurate, but are lighter and faster. A miniature OP-TDL methane sensor developed by NASA for the Mars Curiosity Rover has been recently adapted for use on board drones (Smith et al., 2017). The so-called Open Path Laser Spectrometer (OPLS) is very sensitive (10 ppb), accurate (±1%), lightweight (<150 g) and fast (<0.5 s), and has been reported to detect methane plumes at more than 200 m downwind of the emission source (Smith et al., 2017).

An interesting open-path variant is stand-off or back-scattered TDLAS (sTDLAS), in which both the emitter and detector are placed at the same end of the optical path. The laser beam is emitted towards a distant (<10 m) surface and the backscattered light is collected by a photodiode (Yang et al., 2018) (Fig. 6). In contrast to point-like technologies, sTDLAS detectors measure the integral or cumulative gas concentration (ppm · m) across the light beam, so a single measurement can capture information over a large area that would otherwise require many point measurements. Lightweight (<600 g) instruments, such as the Laser Methane mini

(LMm) by Pergam Suisse AG (Zürich, Switzerland), offer a fast response (0.1 s), and accuracies of 100–1000 ppm · m.

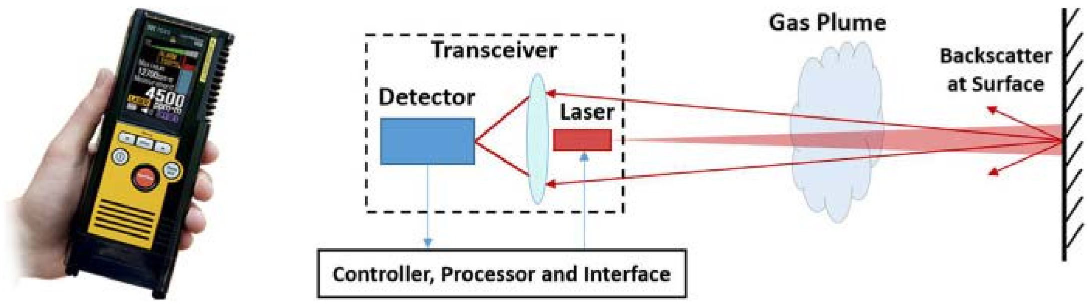


Fig. 6. LMm sTDLAS detector (Pergam Suisse AG) and working principle (Yang et al., 2018).

Cavity enhanced absorption spectroscopy (CEAS) is a group of LAS techniques that use a resonant optical cavity where the laser light bounces back and forth (about 100,000 times), achieving very long effective optical paths of several kilometers (Tittel et al., 2008). Two main CEAS techniques are cavity ring-down spectroscopy (CRDS) and off-axis integrated cavity output spectroscopy (OA-ICOS). Both techniques are extremely sensitive, although to date the instruments have been too heavy and power hungry for drone applications. Recently, lightweight (<4 kg) low-power (<30 W) versions of CRDS and OA-ICOS have been developed that are suitable for drones (Ability, 2019; Martinez et al., 2020). The open-path CRDS instrument developed by Martinez et al. (2020) offers high temporal response (1 s) and high sensitivity (30 ppb), enabling methane plume detection at more than 60 m downwind of the emission source. The OA-ICOS by ABB Group (Zürich, Switzerland) offers sub-ppb sensitivity and response time of only 0.2 s.

### 3.2.5. Optical gas imaging

Optical gas imaging (OGI), also known as backscatter absorption gas imaging (BAGI), is a technique that produces video streams of leaking gases based on the thermal contrast between the background and the gas (McRae and Kulp, 1993). An OGI camera is basically an infrared or thermal imaging camera containing an optical filter tuned to the absorption band of the target gas. If the camera is directed at a scene containing a gas leak with a sufficient temperature contrast (typically >2 °C (Ravikumar et al., 2017)), the gas will 'block' the radiation coming from the objects behind the plume, and the resulting video stream will show the gas plume highlighted over the background (Fig. 7). If atmospheric conditions are favorable (e.g. low wind, warm weather, clear skies) and the imaging distance is lower than 10 m, it is estimated that an OGI camera can detect ~80% of total leakage at a gas production facility (Patel, 2017). The main shortcomings of OGI cameras are their high cost (Ravikumar et al., 2017), the difficulty in quantifying the leak rate (Ravikumar et al., 2018) and the high detection limit (e.g. 10,000 ppm for $CH_4$ (Patel, 2017)).

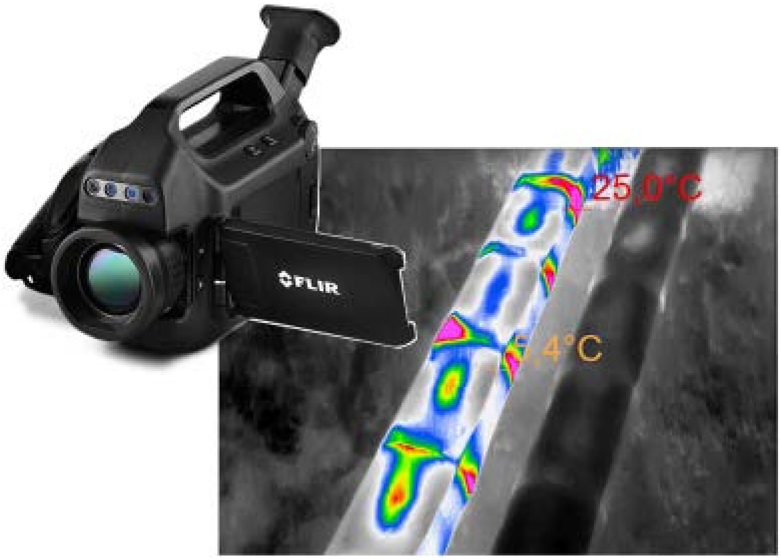


Fig. 7. Visualization of a leaking pipe from an OGI camera (Model: FLIR GF620).

### 3.3. Payload integration

The quality of the measurements acquired by on board chemical instrumentation depends crucially on where they are placed on the drone's fuselage, the type of drone used, the payload characteristics, and the target application.

#### 3.3.1. Rotary-wing drones

The most accurate way for rotorcrafts to take measurements would be to isolate the sensor from the downwash, for example by placing it on a boom extending past the propellers, and thus sampling unperturbed air (Falabella et al., 2018; Goodwin et al., 2009; Smith et al., 2017) (Fig. 8a), or by using a pumped system with an inlet placed away from the platform (Frederiksen and Knudsen, 2018; Kunz et al., 2019; McGonigle et al., 2008) (Fig. 8b–c). Booms are aerodynamically inefficient and displace the center of gravity of the drone, causing stability issues. Pumped systems are more convenient because the payload can be mounted in a centered position either below or above the drone. Most commercial multi-sensor systems use this approach with a ~1 m horizontal sampling tube (e.g. Scentroid DR1000, Aeromon BH-12, and FLIR Muve C360) (Fig. 8b). SnifferRobotics LLC (Ann Arbor, MI, USA) and the SNIFFDRONE prototype (DAM-IBEC, 2019) use a pumped system with a long (~10 m) suspended sampling line (Fig. 8c). The downside of long sampling tubes is that adsorption processes in the inner walls of the tubing can slow the response time for low-volatility or “sticky” compounds, such as H2S or NH3, and can contaminate future measurements.

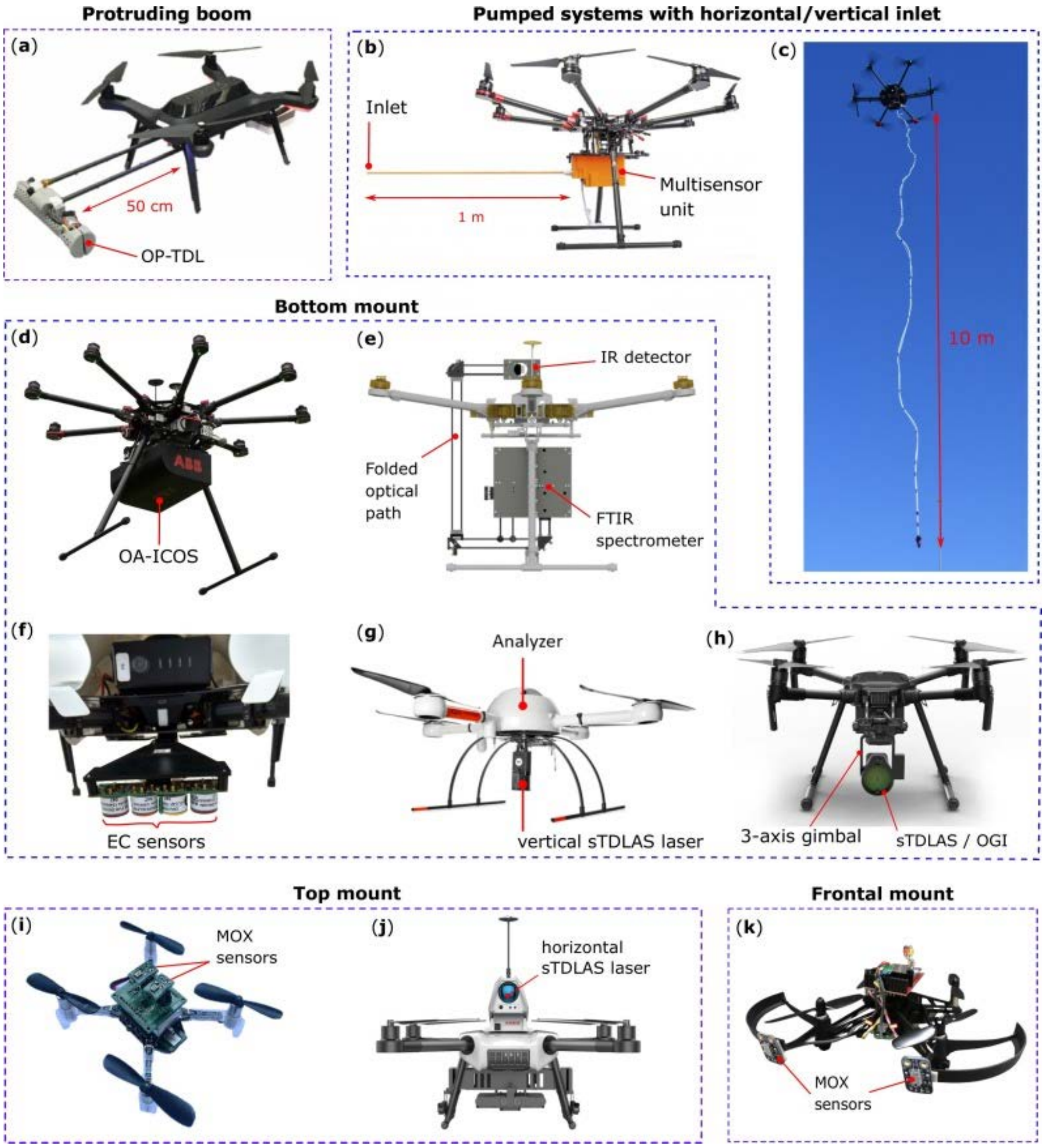


Fig. 8. Integration of chemical instrumentation into RW drones. (a) JPL's open-path TDL mounted in a 3DR Solo using a boom (Smith et al., 2017); (b) DJI Matrice 600 mounting Scentroid's DR1000 multi-sensor unit with a horizontal sampling inlet; (c) DJI Matrice 600 with custom multi-sensor system and vertical sampling inlet (DAM-IBEC, 2019). (d) DJI S1000 with integrated OA-ICOS analyzer (ABB Group); (e) Schematic representation of a FTIR spectrometer integrated into a DJI Matrice 600 using a C-shaped optical path of 1 m (Rutkauskas et al., 2019); (f) Four AGS sensors mounted beneath a DJI Matrice 100 (de Man, 2018); (g) Microdrones' md1000 equipped with downward-facing sTDLAS detector (LMm by Pergam Suisse AG); (h) DJI Matrice 210 with U10 sTDLAS analyzer (AILF Instruments, China) mounted on the 3-axis gimbal plate; (i) CrazyFlie 2.0 nanodrone with two replicate MOX sensors on top of it (Burgués et al., 2019a); (j) Hesai DM100 drone with integrated sTDLAS detector above the drone; (k) Pocket-sized quadcopter (Parrot Airborne Nightblaze) mounting two replicate MOX sensors in front of the propellers (Shigaki et al., 2018).

For simplicity, many research prototypes have the payload mounted in a central position below (de Man, 2018; Kersnovski et al., 2017; Pobkrut et al., 2016; Rossi et al., 2014; Wivou et al., 2016; Yang et al., 2017) (Fig. 8d–h) or above (Alvear et al., 2017; Burgués et al., 2019a; Hutchinson et al., 2019; Qiu et al., 2017; Roldán et al., 2015) (Fig. 8i–j) the fuselage, with no pumping system to isolate it from the downwash. While this does not create a problem for long-range sensors such as sTDLAS or OGI cameras, point sensors installed in this way typically underestimate the gas concentration (Hutchinson et al., 2018; Neumann et al., 2012; Poppa et al., 2013; Roldán et al., 2015; Valente et al., 2019). Rutkauskas et al. (2019) created an intelligent integration solution for a Fourier Transform Infrared (FTIR) spectrometer, in which they folded the optical path in a C-shape around the drone (Fig. 8e), attached the heaviest components (i.e. IR source and mirrors) underneath, and those more affected by the downwash (i.e. the IR detector) above, where airflow disturbance is much lower. Top- and front-mounting (Fig. 8i–k) is very popular for GSL applications (see Section 4.2), in which it is more important to rapidly detect the gas plume than to accurately quantify the gas concentration. For this purpose, pairs of replicate MOX sensors are often placed on the front of small quadrotors (Koval et al., 2017; Kuantama et al., 2019; Letheren et al., 2016; Shigaki et al., 2018; Takei et al., 2019) (Fig. 8k), or in more complex configurations such as three sensors placed in a triangle arrangement (Luo et al., 2017) or four sensors below the propellers (Eu and Yap, 2018).

The bottom mounting is very convenient for sTDLAS sensors in surface emission monitoring (SEM) applications because the laser can be pointed towards the ground to produce column integral measurements (Fig. 8g). This configuration is adopted by several companies, such as Microdrones GmbH (Siegen, Germany), SPH Engineering (Riga, Latvia) and Baker Hughes (Texas, USA), and also by different research groups (Emran et al., 2017; Golston et al., 2018a; Oberle et al., 2019; Tannant et al., 2018; Yang et al., 2018). The 3-axis gimbal plate (Fig. 8h) is also an interesting mounting location for long-range sensors (sTDLAS and OGI cameras), as it allows them to be rotated in any direction. This approach has been commercialized by multiple companies including DJI (Shenzhen, China), Viper Drones (Indialantic, FL, USA), RMUS (Centerville, UT, USA), Baker Hughes (Houston, TX, USA) and Sky Eye Innovation (Stockholm, Sweden).

### 3.3.2. Fixed-wing drones

The slow response time of most chemical sensors is incompatible with the high speed of FW drones, with the exception of OP-TDL detectors, whose response times can be as low as 0.1 s. These sensors can be mounted on the nose (Fig. 9a–b) (Hollenbeck et al., 2019a; Nathan et al., 2015) or under the wings of FW platforms (Golston et al., 2017) to sample undisturbed air during forward flight. An interesting integration idea presented by Barchyn et al. (2017) consists of creating an optical path between the winglets (Fig. 9c) by using fiber optic cable to locate the emitter and detector at a distance from the sending and receiving optics (housed inside the fuselage).

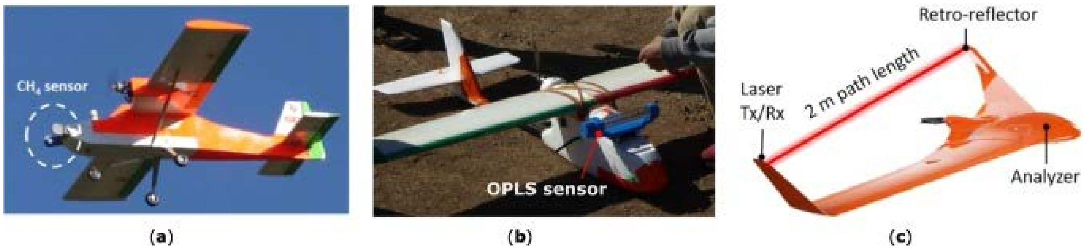


Fig. 9. Open-path tunable diode laser (OP-TDL) methane detectors mounted on FW drones; (a) Custom OP-TDL sensor mounted on the nose of a model aircraft. Reprinted with permission from Nathan et al. (2015). Copyright 2015 American Chemical Society; (b) JPL's OP-TDL sensor installed on top of the nose of a 3DR AeroM drone. Courtesy of Derek Hollenbeck; (c) Bramor PPX aircraft (C-Astral Aerospace Ltd.) with integrated OP-TDL sensor by Boreal Laser Inc.

Adapted with permission from C-Astral Aerospace.

### 3.4. In-flight sensor performance

The issues that affect the performance of sensors on board a drone are not very different from those encountered by fixed gas detectors in the field. Uncontrolled or unknown variations in temperature, humidity, and pressure can obviously affect the sensor signals, as can overheating due to direct sunlight exposure. Strong winds also affect sensor signals, especially if the sensors are not isolated. While fixed detectors can be shielded against direct sunlight and precipitation, this is difficult to achieve in drones because they can rotate in any direction. All these factors clearly affect the accuracy and sensitivity of the sensor, which can eventually dictate the success of the mission.

#### 3.4.1. Response time

The response time of the chemical sensing instrument is a key parameter for drone-based measurements, as it dictates the maximum speed at which the drone can fly while still obtaining spatially resolved measurements. In this sense, the fastest type of sensor is the sTDLAS, which can sample at a frequency of 10 Hz and is not affected by the downwash (Emran et al., 2017). This means that a drone flying at a relatively high speed of 10 m/s could achieve a spatial resolution of 1 m. Other open-path optical sensors can measure at 1–5 Hz (Ability, 2019; Barchyn et al., 2019; Martinez et al., 2020; Rutkauskas et al., 2019). Low-cost sensors integrated directly into the drone without any pumped system typically offer bandwidths of 0.1 Hz, although the response time can be improved by signal processing (Burgués and Marco, 2020, Burgués and Marco, 2019; Martinez et al., 2019). In pumped systems, including closed-path optical analyzers, the response time is mostly determined by the volume of the measurement chamber and the flow rate of the pump, and is commonly about 1 min for a typical pumped system with a chamber volume of 200–300 cm3 and a flow rate of 1–2 L/min. In this case, a common solution for increasing the spatial resolution of the measurements is to hover the drone briefly at each sampling point (e.g. 20–30 s) before proceeding to the next sampling point (Neumann et al., 2012). Memory effects due to contamination of the sampling line may also degrade the system's response time.

### 3.4.2. Limit of detection

The limit of detection (LOD) of a chemical sensor refers to the minimum concentration of the target gas that can be reliably distinguished from the absence of the same gas (Burgués et al., 2018). The LOD is very important for drone-based measurements as it determines the maximum downwind distance at which the chemical plume can be detected. The LOD is usually estimated as three times the standard deviation of the sensor's baseline noise (Danzer and Currie, 1998). The LOD reported in sensor datasheets is usually estimated in highly controlled laboratory conditions where temperature, pressure, and humidity are fixed and there are no interfering gases. When a chemical sensor is used in a drone and operated in uncontrolled outdoor conditions, several factors will degrade its LOD. First, if the downwash of the propellers is not properly avoided, this will dilute the gas reaching the sensor and thus increase the LOD (Neumann et al., 2012). Large fluctuations in temperature, humidity and pressure will increase the LOD of most sensor systems, unless these fluctuations are actively compensated for. Finally, vibration and misalignment will affect most optical analyzers, especially those with long effective pathlengths (Martinez et al., 2020). Even with these considerations, some high-end optical analyzers have been shown to achieve in-flight LODs of ~15–30 ppb (Martinez et al., 2020).

### 3.4.3. Dynamic range

Unlike fixed gas detection systems, which are typically placed at a convenient downwind distance from a potential chemical source, drones can be flown very close to the source and very far from it, even in the same application. For example, in odor emission monitoring applications, the drone can start measuring at the receptor site (where concentrations are on the order of ppb), and progressively move towards the source (where concentrations can reach thousands of ppm's). This scenario would require a sensor with a dynamic range covering more than seven orders of magnitude in gas concentration, which is difficult to achieve in practice. Instruments optimized for measuring low ppb concentrations, such as the OA-ICOS or CRDS analyzers, typically employ long effective optical paths that clip the sensor signal when absorbance gets too high (zero light detected). Similarly, electrochemical sensors have relatively low maximum ratings, making them inappropriate for measurements at the source of emission. In the case of ammonia, most electrochemical sensors have a maximum rating of 100 ppm, above which they become irreversibly damaged.

## 4. Tasks and algorithms

Beyond the simple task of monitoring the gas concentration at a certain location, small drones can perform four "advanced" chemical sensing tasks: concentration mapping, source localization, source identification, and flux quantification. In this section, we explain the different algorithms developed to address these tasks.

### 4.1. Gas concentration mapping

Gas concentration mapping (GCM) is the task of building a spatial representation (i.e. a map) of gas concentrations in a certain area based on a set of spatially distributed sensor measurements (Fig. 10). Such a map is useful for assessing the spread of a target gas, e.g. in the aftermath of a chemical accident or for air quality monitoring in cities, and as an indirect tool for localizing gas sources (Section 4.2) and estimating gas fluxes (Section 4.3). To build a gas distribution map, the drone typically follows a predefined navigation path with equidistant measurement points at which it stops for a few seconds to measure the gas concentration. A common method for generalising the point-wise measurements is spatial interpolation (Lam, 1983), for example using Gaussian kernels (Lilienthal and Duckett, 2004), polynomial functions (Keys, 1981), or natural neighbor techniques (Sibson, 1981). The rationale behind spatial interpolation is that points close together in space are more likely to have similar values than points far apart. Due to the inherent uncertainty in the measured values, it is preferable to use smoothing interpolators (as opposed to exact interpolators) as this reduces the effects of measurement error on the interpolated surface.

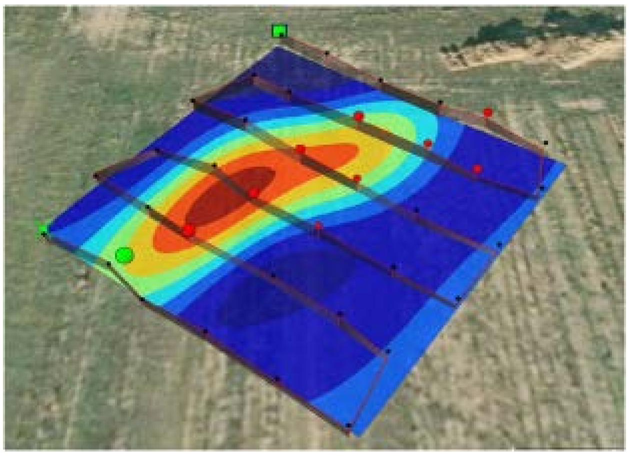

Fig. 10. Two-dimensional gas concentration map of a 25 m × 25 m outdoor area. Measurements at equidistant grid points were obtained with a DJI Matrice 100 equipped with a PID sensor, and flying at constant height (Personal communication from Michael Hutchinson).

Drone-based GCM was initially performed using blimps equipped with MOX sensors for 2D mapping of controlled releases of ethanol vapor in indoor (Ishida, 2009) and outdoor (Badia et al., 2007) areas. More recently, GCM has been performed in less controlled and larger environments, such as farmyards (Rutkauskas et al., 2019), greenhouses (Roldán et al., 2015) and landfills (Emran et al., 2017), using small RW drones equipped with a variety of sensing technologies (see Table S2 in Supplementary material). There have also been some reports of 3D mapping strategies (Burgués et al., 2019a; Li et al., 2017; Luo et al., 2015) and multi-source experiments (Rutkauskas et al., 2019). To speed up the map-building process, some authors have used multiple collaborative drones (He et al., 2019) or adaptive path planning strategies (Neumann et al., 2012), or have performed measurements in motion (Burgués et al., 2019a; Li et al., 2017; Luo et al., 2015; Rutkauskas et al., 2019).

GCM based on integral path measurements from sTDLAS detectors is a promising approach because (i) the long-range measurements can be performed at sufficient distance so that the downwash does not disturb the gas distribution being mapped; (ii) the detector's high sampling frequency enables rapid mapping of large areas; and (iii) the resulting map captures the cumulative concentration in the vertical direction without the need for (costly and time-intensive) 3D sampling. In this regard, several studies (Emran et al., 2017; Golston et al., 2018a; Tannant et al., 2018; Yang et al., 2018) used small quadrotors equipped with downward-facing sTDLAS detectors to map CH4 concentrations in controlled leak experiments (Golston et al., 2018a; Tannant et al., 2018; Yang et al., 2018) and landfill sites (Emran et al., 2017). In all cases, the drone flies at a constant height of <10 m (at greater heights the measurements become unreliable (Tannant et al., 2018)) while emitting the laser beam towards the ground and receiving the backscattered light. The resulting maps clearly indicate the location of CH4 emission hotspots. Taking a different approach, Neumann et al. (Neumann et al., 2019) performed gas tomography (Price et al., 2001)—a method for reconstructing 2D slices of the gas distribution from path-integral data—using a sTDLAS detector mounted on a 3-axis gimbal of an octocopter. Instead of performing one path-integrated measurement at each sampling location, the detector emits multiple beams towards the ground at different angles. After collecting samples in many different locations, a least-squares optimization algorithm (Trincavelli et al., 2012) is used to solve the inverse problem of determining the spatial distribution of gas concentrations that best explains the observed integral measurements.

### 4.2. Gas source localization

Gas source localization (GSL) consists of finding the source of an emitted chemical based on the chemosensory cues available in the environment. It has numerous applications, such as finding gas leaks in industrial sites, locating the source of a malodor, or locating survivors following a natural disaster. In many of these scenarios, the chemicals released are dispersed by wind in the form of a plume that may extend several km downwind of the source (Fig. 11). Reactive plume tracking (RPT) strategies (Chen and Huang, 2019; Kowadlo and Russell, 2008) use concentration and wind measurements to track the plume towards its origin, inspired by the excellent plume tracking behavior of some insects (Mafra-Neto and Cardé, 1994). Both 2D and 3D versions of RPT algorithms have been evaluated using small rotorcrafts equipped with MOX sensors, resulting in success rates of >70%, albeit in very simplified test conditions (see Table S3 in Supplementary material). These favorable conditions include forcing a strong unidirectional air flow to create a well-shaped plume, restricting the search space to a few m2, placing the drone in advantageous starting positions, or declaring that the source has been found as soon as the drone passes near it. In more realistic scenarios, RPT algorithms have proven much less successful due to unpredictable wind patterns and the limitations of current sensing and locomotion technologies (Hernandez Bennetts et al., 2012b).

Fig. 11. Time-averaged chemical plume emitted by an industrial site and reaching a nearby population. The plume is simulated using CALPUFF dispersion modelling (Scire et al., 2000). Personal communication from ATTRACT-SNIFFDRONE project.

Instead of reactively tracking the plume, probabilistic (plume modelling) algorithms assume a plume dispersion model and use local measurements of concentration and wind to fit the model and estimate the source location (a parameter of the model). Any relevant atmospheric model can be used, such as Gaussian Plume (Bakkum and Duijm, 1997), isotropic (Hutchinson et al., 2019; Vergassola et al., 2007), filament-based (Farrell et al., 2002), or even CFD models (Asenov et al., 2019). A Bayesian inference framework is typically used to recursively estimate the source parameters given a sequence of observed measurements (Farrell et al., 2003; Hutchinson et al., 2019; Pomareda et al., 2017; Vergassola et al., 2007). The navigation strategy is often based on an exploration-exploitation trade-off. One of the most widely known algorithms in this category is Infotaxis (Vergassola et al., 2007), which was recently extended to 3D (Ruddick et al., 2018). Probabilistic algorithms have been recently tested on RW drones to find gas leaks in relatively large outdoor areas (>1000 m2), achieving localization errors of <20 m (Asenov et al., 2019; Hutchinson et al., 2019).

### 4.3. Gas source identification

Gas source identification consists of deciding whether a candidate source is currently emitting a chemical or not. This is a much simpler problem than gas source localization, as the location of the potential gas sources is known in advance. For example, Qiu et al. (2017) tried to predict the active chemical source from a set of five candidate sources in a chemical industry park (4 km2). Assuming a Gaussian plume model, they trained an artificial neural network (ANN) with simulated data under different wind conditions. The method was validated in field experiments by flying a RW drone equipped with MOX sensors around the perimeter of the park, correctly identifying the emitting source.

### 4.4. Gas flux quantification

For some applications, it is not sufficient to simply localise/identify an emitting source, but rather there is a need to quantify the emission rate (e.g. kg of gas released per hour). For example, refineries and petrochemical plants are required not only to detect and repair leaks, but also to quantify the total amount of methane released by fugitive emissions for inventory purposes. Other scenarios such as landfills require the plant operator to report whole-site emissions periodically. Recent studies have explored the feasibility of using drone-based measurements for on-site and off-site quantification of methane emissions from oil and gas infrastructure and landfills. The most common flux estimation method for small drones is the mass balance method (Allen et al., 2018), which derives the net flux by integrating the measured concentration (above background level) across a vertical sampling plane downwind of the emitting source (Fig. 12), and multiplying the result by the wind speed (m/s) perpendicular to that plane. This method has been applied to estimate whole-site CH4 emissions from natural gas infrastructure (Nathan et al., 2015) and landfills (Allen et al., 2018), using data captured by FW drones downwind of these sites. These experiments were uncontrolled, which precludes a rigorous validation of this method's accuracy, and errors of at least a factor of 3 are likely (Nathan et al., 2015).

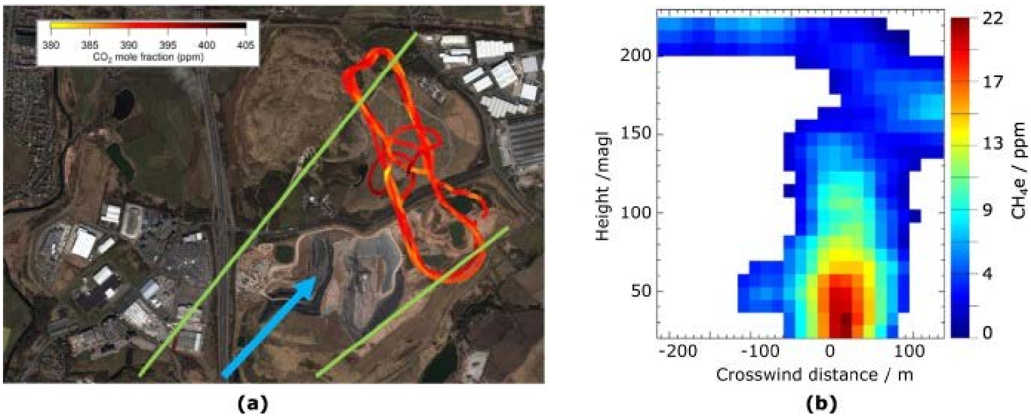


Fig. 12. Flux quantification using the mass-balance method for FW drone flights (Allen et al., 2018). (a) Flight track at 510 m downwind of the emission source (landfill). A blue arrow shows mean wind direction and green lines illustrate the expected landfill plume extent; (b) Methane enhancement (CH4e) over background, spatially interpolated onto a 2D flux vertical plane. (For interpretation of the references to color in this figure legend, the reader is referred to the web version of this article.)

Yang and Golston (Golston et al., 2018a; Yang et al., 2018) proposed a new application of this method, tailored for near-source sampling using small rotorcrafts equipped with downward facing sTDLAS instruments. Their approach first uses the drone to build a vertically-integrated gas concentration map around the leak source, and then rotates this map so that the x-axis is aligned with the crosswind direction (Fig. 13a). Since measurements are already integrated in the vertical direction, the mass balance can be computed by integrating the map in the crosswind direction (Fig. 13b) and multiplying by the wind speed. The leak rate is estimated as the 95th percentile of the crosswind integrated flux (dashed line in Fig. 13b). Tests performed in the context of controlled methane release yielded quantification errors of 0.05 g/s ± 25% of the true emission rate (0–0.17 g/s). These results may appear inconsistent with those of a recent systematic, blind intercomparison experiment (Ravikumar et al., 2019), where RW drones equipped with optical detectors were only able to quantify leaks with an order-of-magnitude (0.1–10x) error with respect to the metered leak rate, although this discrepancy may be due to the challenging nature of blind experiments.

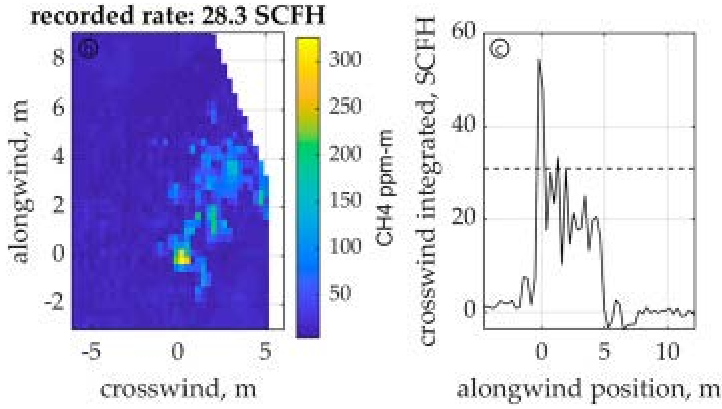


Fig. 13. On-site flux quantification algorithm based on the mass balance approach applied to path-integral measurements from a small quadrotor (Golston et al., 2018b). (a) Rotated gas concentration map of path integral data (ppm · m); (b) Crosswind integrated flux. The horizontal dashed line indicates the 95% percentile of the data, which is the final estimation of the leak rate.

A second class of methods, the so-called plume model inversion methods, assume a particular plume dispersion model and try to estimate the release rate (a parameter of the model) by fitting this model with measurements of gas concentration and wind. Inverse methods based on Gaussian, Lagrangian, and isotropic models have been tested using measurements from FW and RW drones in controlled and uncontrolled methane releases (see Table S4 in the Supplementary material). Tests based on the Gaussian model gave relative estimation errors of ~250% when gas concentration measurements where obtained by a ground-based OA-ICOS analyzer tethered to a RW drone (which was used to fly the inlet of a long sampling tube) (Shah et al., 2019a), and even larger errors when using an on-board NDIR analyzer (Shah et al., 2019b). Hutchinson et al. (2019) used an isotropic plume model to quantify a controlled release of acetone (1.5 g/s) in an outdoor field. Concentration measurements were taken with a PID mounted on a quadrotor, and wind measurements came from a meteorological station. In 10 trials, estimated fluxes ranged from 1.59 to 2.75 g/s, representing a relative error of 10–83% of the true leak rate. Xi et al. (2016) used an inverse Lagrangian model—the so-called Stochastic Time-Inverted Lagrangian Transport (STILT) model—coupled with high resolution meteorological data from a numerical weather prediction model to quantify the SO2 emission flux from a volcanic plume. They validated the time-averaged wind speed predictions simulated by the weather model using experimental data from two nearby meteorological stations.

**5. Applications**

Current applications of small drones can be divided into five groups: (i) atmospheric chemistry research, (ii) industrial emission monitoring, (iii) law enforcement, (iv) safety and security, and (v) precision agriculture (Fig. 14).

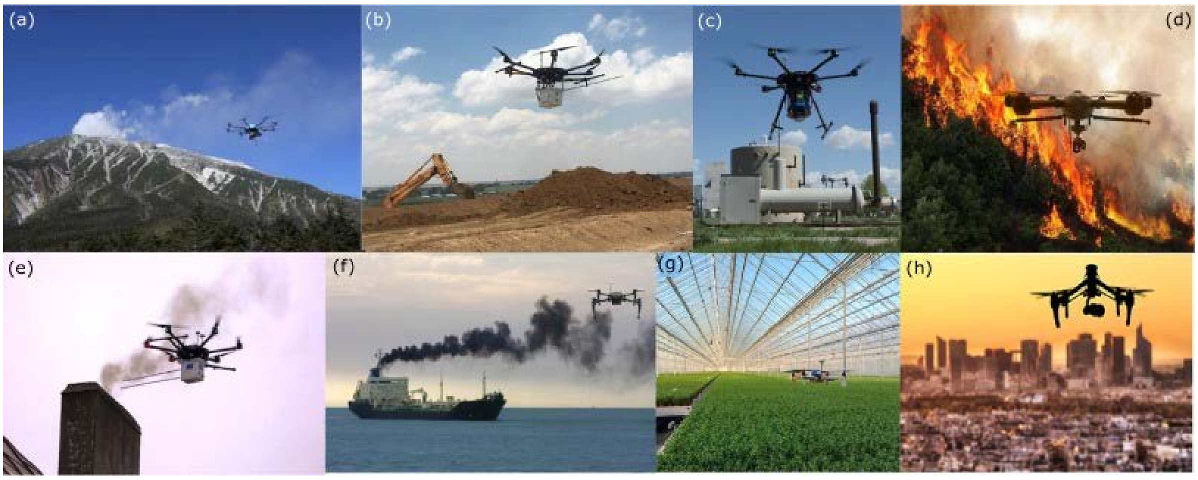

Fig. 14. Applications of small drones equipped with chemical instrumentation. (a) volcanic research (Mori et al., 2016); (b) landfill emission monitoring (Reproduced with permission from Scentroid); (c) methane monitoring in industrial sites (Photo by Sean Boggs/Environmental Defense Fund); (d) early fire detection; (e) residential emissions monitoring (Reproduced with permission from Scentroid); (f) ship emission monitoring (Photo: NERC); (g) precision agriculture (Reproduced with permission from Applied Drone Innovations B.V.); (h) urban air quality (Photo: Digital Trends).

### 5.1. Atmospheric chemistry research

Instrumented drones can provide experimental measurements of atmospheric constituents (e.g. CH4, CO2, NOx and O3) and thermodynamic variables (temperature, humidity, pressure, wind, etc.) in the lower troposphere. These measurements have a much lower cost than manned aircraft, blimps or balloons, and can be taken over a wider spatial region than fixed monitoring stations or towers, and at higher spatial resolution than satellite-based measurements. In the last 15 years, small drones have been used to capture vertical and horizontal profiles of GHGs (Brady et al., 2016; Brosy et al., 2017; Golston et al., 2017; Gramm and Schütze, 2003; Khan et al., 2012a; Khan et al., 2012b; Kunz et al., 2019; Malaver Rojas et al., 2015; Nathan et al., 2015; Schuyler and Guzman, 2017; Schuyler et al., 2019; Watai et al., 2006) and ozone (O3) (Baxter and Bush, 2014; Li et al., 2017) in the atmospheric boundary layer (ABL). In their pioneering work, Watai et al. (2006) used a gasoline-powered FW drone equipped with an NDIR sensor to explore CO2 variations up to a height of 2000 m. More recently, NDIR sensors mounted on RW drones have been used to measure the surface flux of CO2 (Kunz et al., 2019, Kunz et al., 2018). Several authors (Golston et al., 2017; Schuyler et al., 2019) have exploited the ability of FW and RW drones to fly horizontally and vertically, respectively, to explore vertical and horizontal variation in GHGs and thermodynamic variables in the ABL (Fig. 15). While Golston et al. (2017) used custom OP-TDL sensors, Schuyler et al. (2019) used low-cost chemical sensors, correcting the result for the effects of temperature at different relative humidities. Brosy et al. (2017) studied the nocturnal evolution of vertical profiles of methane of up to 50 m above ground level using a RW drone tethered to a ground-based CRDS.

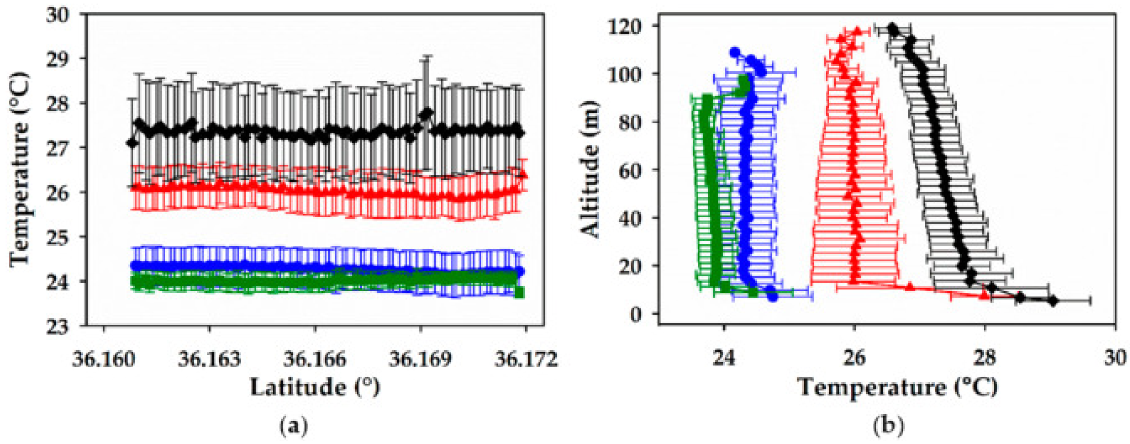


Fig. 15. Diurnal variation in the (a) horizontal and (b) vertical profiles of atmospheric temperature for the times (green square) 6:04–6:56 a.m., (blue circle) 7:06–7:57 a.m., (red triangle) 8:11–9:05 a.m., and (black diamond) 9:28–10:22 a.m. Data was captured with a RW drone (Schuyler et al., 2019). (For interpretation of the references to color in this figure legend, the reader is referred to the web version of this article.)

Drones are also an excellent platform for volcanic plume sensing, as they can carry gas detectors and samplers directly into the plume, minimizing risk to humans. The main reason for studying emissions from volcanoes is the concern about the environmental effects of volcanic gases, particularly acid rain caused by SO2 and the "greenhouse" effects of CO2 emissions (Hards, 2005; Robock, 2000). Plume measurements provide a better understanding of how and why volcanoes erupt (von Glasow et al., 2009), and allow geologists to diagnose underground magma conditions for eruption forecasting (McGonigle et al., 2008). Thus, periodic monitoring of volcanic gases can be used to prepare communities for volcanic eruptions (Muscato et al., 2012), and mitigate ash hazards for aviation (Diaz et al., 2015). Several research missions have used RW drones to carry chemical sensors into volcanic plumes to measure the CO2/SO2 ratio (McGonigle et al., 2008; Rüdiger et al., 2018), analyze the composition of fumaroles following eruptions (Mori et al., 2016; Shinohara, 2013), investigate the dynamics of volcanic outgassing and plume transport (Liu et al., 2019), and quantify SO2 emission rates (Xi et al., 2016). In a collaborative project between NASA and University of Costa Rica (Diaz et al., 2015; Pieri et al., 2013), a miniaturized mass spectrometer (MMS) was flown into a volcanic plume to perform a detailed composition analysis (Fig. 16). This represents a significant advance in the state of the art of airborne gas measurement, i.e. using a drone to collect laboratory-quality data directly in the field.

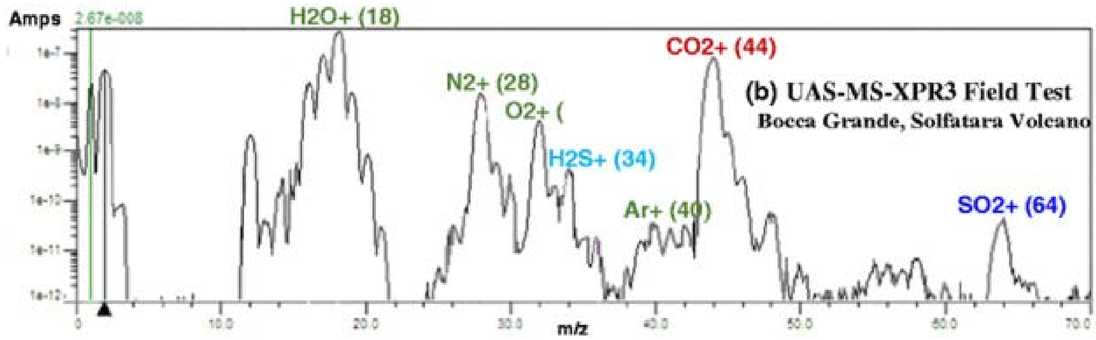


Fig. 16. Mass spectrum of a volcanic plume captured with a miniaturized mass spectrometer (MMS) on board of a RW drone. The spectrum reveals the presence of H2O and CO2 as main gases, H2S and SO2 as trace gases (tens of ppm) and some air contamination (N2, O2 and Ar peaks).

Reproduced with permission from Diaz et al. (2015).

Wildfires and thawing permafrost are also important sources of GHGs and pollutants. Wildfires are estimated to account for 5–10% of annual global CO2 emissions (Knorr et al., 2016), while methane escaping from thawing permafrost in Artic regions accounts for 3.5% of global CH4 emissions (Schuur et al., 2015). Measuring these emissions allows us to predict exposure and estimate risks to human health and the environment, and to reinforce emission inventory calculations (Aurell and Gullett, 2013). To explore the feasibility of using drones for such measurements, Zhou et al. (2017) used a RW drone equipped with low-cost CO and CO2 sensors to derive carbon emission factors in a smoke plume simulating a wildfire. More recently, Oberle et al. (2019) used a RW drone equipped with a downward-facing sTDLAS analyzer to map surface emissions of methane in the Artic, successfully identifying potential locations of thawing permafrost.

### 5.2. Industrial emission monitoring

Emissions of gaseous pollutants, odor and dust are still unavoidable in certain industrial activities today despite a wide range of abatement options are available. This can lead to disruptions from environmental permit requirements, fines, and can impact on nearby communities which results in poor publicity in the media and damaged reputation. Characterizing and monitoring the environmental impact of an industrial plant is key for preventing and reducing industrial pollution, and minimizing impact to surrounding population. In this line, drones equipped with chemical detectors can supplement the information provided by continuous emission monitoring systems (CEMS) typically installed on the plant, and periodic walkover surveys with hand-held detectors. Drones can provide measurements with much better spatial resolution than fixed detectors, and with less risk than walkover surveys.

In many countries, emission monitoring is mandatory for certain industries to assess compliance with environmental permit requirements. For instance, atmospheric emissions in Europe are regulated by the Industrial Emissions Directive 2010/75/EU (IED), which specifies the gases that require monitoring and the recommended measurement method for each gas. The most common gases that require measurement are combustion gases (i.e. SO2, NOx and CO), VOCs and acid gases such as HCl, HF, and NH3. This IED states that while measurement techniques based on transportable measurement platforms may be less accurate than reference methods (typically laser-based optical analyzers), they may be used to supplement information from fixed measurements in order to determine spatial concentration distributions. This encourages the use of drones to map air pollutants over a specific area of an industrial plant, or across the entire plant, in order to find fugitive emissions, help validate mathematical emission models, and control effectiveness of abatement measures.

Refineries and petrochemical plants emit 600–700 tons/year of hazardous gases (mostly $CH_4$) and VOCs from leaking equipment, such as valves, connectors, or open-ended lines (United States Environmental Protection Agency (EPA), n.d.). As a result, these industries must conduct periodic Leak Detection and Repair (LDAR) surveys to minimize gas leaks. Aerial surveys by drones equipped with methane detectors are a promising cost-effective alternative to current walkover LDAR inspections. Fixed-wing platforms equipped with TDLAS detectors were initially assessed for leak detection (Barchyn et al., 2017; Hollenbeck et al., 2019a) and whole-site emission quantification (Nathan et al., 2015), but with limited success. More recently, these tasks have been tackled using RW drones equipped with OP-TDL detectors (Smith et al., 2017; Whitehead, 2018; Whiticar et al., 2019, Whiticar et al., 2018) and downward facing sTDLAS instruments (Golston et al., 2018a; Yang et al., 2018). A recent systematic, blind experiment at a gas production site showed that RW drones equipped with OP-TDL sensors were capable of accurately (>80%) identifying leaking equipment (Ravikumar et al., 2019). Indeed, many important O&G companies, such as ConocoPhillips (2019), TOTAL Group (2019) or BPX-Energy (2019), are already testing this technology at their plants.

Waste treatment sites, such as SWLs and WWTPs, are major sources of GHGs and offensive odors. Landfill gas is composed of ~50% $CH_4$ and ~50% $CO_2$ (Lou and Nair, 2009), whereas WWTP emissions are mostly composed of $CH_4$ and $N_2O$ (Daelman et al., 2013). Operators of large SWLs and WWTPs are required to provide annual reports on the emission of hazardous compounds that exceed permissible levels (United Nations Economic Commission for Europe (UNECE), 2008). Recently, research groups and companies have deployed drones in SWLs for surface emissions monitoring (SEM), as an alternative to traditional measurement techniques such as walkover surveys and surface flux chambers. For instance, Sniffer Robotics LLC (USA) addresses SEM monitoring using a RW drone equipped with a CP-TDL detector connected to a long sampling tube with a sampling inlet suspended at 5–10 cm above the ground. In this type of scenario, however, a more elegant solution that does not require long sampling tubes is to equip the drone with a downward facing sTDLAS instrument (Emran et al., 2017). Both approaches are effective for mapping the surface methane concentration, highlighting the most important emission hotspots (Fig. 17), and this information is key for the landfill operator to implement abatement solutions.

Fig. 17. Surface methane map of a landfill site captured by a RW drone mounting a CP-TDL methane sensor and a 10-m vertical sampling inlet. Permission granted by Sniffer Robotics, LLC.

In the case of WWTPs, odorous compounds produced by wastewater treatment, such as NH3, H2S or mercaptans, represent an important annoyance problem for workers and communities living near these facilities (Aatamila et al., 2010; Palmiotto et al., 2014). Current odor assessment methodologies use costly and infrequent olfactometry measurements involving human panels, leading to poor temporal and spatial resolution (Bax et al., 2020). The idea of using a drone equipped with chemical sensors to monitor malodors in WWTPs was originally devised by Lega and Napoli (2008), but was not tested in practise. Currently, the European project SNIFFDRONE is exploring the feasibility of using a RW drone equipped with an e-nose to map offensive odors in WWTPs (DAM-IBEC, 2019). The drone also integrates a vacuum sampling device to grab ambient air samples into 10-L nalophan bags, which are analyzed by dynamic olfactometry to calibrate and validate the e-nose predictions.

Mining operations at open-pit mines can damage the environment and the health of surrounding populations due to emissions of dust particles and gases such as CH4, CO2, NOx, and SOx (Alvarado et al., 2015). In particular, blasting operations inject plumes of concentrated NOx (500 ppm) and PM (400 µg m−3) into the atmosphere at concentrations that can exceed local safe limits by up to 3000 fold (Oluwoye et al., 2017). Alvarado et al. (2015) and Bui et al. (2019) proposed to use drones equipped with optical particle counters (OPCs) and low-cost air quality sensors to monitor dust, NO2, NO and CO at open-pit mining sites, as an alternative to ground-based samplers and open-path analyzers. While the work by Alvarado et al. (2015) was a feasibility study carried out in an open field using talcum powder as a dust source, the experiments by Bui et al. (2019) were carried out in a real open-pit mine, in which they flew the drone in a circular pattern at an altitude of 120 m to map the concentration of several pollutants.

### 5.3. Law enforcement

Drones are also a useful measurement platform for environmental agencies and police departments to ensure compliance with air emission regulations. Maritime authorities in Netherlands, Denmark (Explicit-ApS, 2017), Norway, and Hong-Kong (Topali and Psaraftis, 2019) have begun to use drones to check ships coming into and out of their ports for compliance with the fuel sulfur content (FSC) emissions regulations established by the International Maritime Organization (IMO) (Eyring et al., 2010). Previous inspection methods were limited to examining the ship's log books, visually assessing smoke opacity, or manually analyzing fuel samples from random ships. In contrast, a drone equipped with SO2 and CO2 sensors requires only 2 min of hovering within the plume of a ship to ascertain the FSC with reported accuracy of 0.03% (Zhou et al., 2019). If high sulfur levels are detected, an oil sample can be taken from the ship when it is in port to confirm the results and report them to the police.

Emissions from residential heating are also a major source of outdoor air pollution worldwide (Rehfuess, 2006), especially in some developing countries where it is common for people to heat their homes with low-quality coal, scrap wood, and even garbage. In many cases this has become illegal under new environmental laws, so police officers have begun to use drones equipped with AGS and MOX sensors to “sniff” chimneys in residential neighborhoods to test for elevated concentrations of Ethanol, Formaldehyde, Ammonia, or Hydrogen Chloride, as these chemicals indicate the use of low-quality burning material (Scentroid, 2018).

### 5.4. Safety and security

Thanks to their rapid deployment, drones are promising tools for safety and security applications, such as early fire detection, or search and rescue. Drones equipped with chemical sensors can overcome some of the limitations of camera-based drones currently used by fire departments to detect uncontrolled fires. One problem of image-based systems is that they can only detect fires at advanced stages, e.g. when there is already a flame or a large smoke column, which introduces a detection delay. Another problem is false positives caused by phenomena with similar characteristics to flame or smoke, such as sunlight, dust, fog, or water plumes (Krüll et al., 2012; Yuan et al., 2015). MOX sensors and PIDs can assist early fire detection by detecting VOCs released in the pyrolysis and smoldering stages of a fire (Fonollosa et al., 2018; Krüll et al., 2012). They can also be used to confirm a candidate fire detected by a camera (Krüll et al., 2012; Von Wahl et al., 2010).

Other scenarios for gas-sensitive microdrones include detecting dangerous gases and locating unconscious victims in buildings that have collapsed due to earthquakes or explosions. In these situations, rescue teams usually bring hand-held gas detectors to find gas leaks, and trained dogs to search for victims, and these resources could be supplemented with drones equipped with cameras and gas sensors. Such drones would expand the possibilities for emergency crews, who could thus fly the drone throughout indoor spaces, overcoming obstacles such as stairs and debris. As a proof of concept, a recent study demonstrated the use of a nano-drone (weighing just 35 g) for indoor gas source localization and mapping (Burgués et al., 2019a).

### 5.5. Precision agriculture

Drones equipped with environmental sensors have been proposed as an option to automate certain agricultural tasks, such as monitoring climate variables in greenhouses or assessing fruit maturity. Roldán et al. (2015) used a quadrotor to produce high-resolution maps of air temperature, humidity, luminosity and CO2 in a greenhouse. In a follow-up study (Roldán et al., 2016), they proposed a multi-robot system consisting of an unmanned ground vehicle (UGV) carrying a small drone, which combines the robustness and autonomy of the UGV for continuous work with the agility and speed of the microdrone for occasional interventions.

Valente et al. (2019) studied the feasibility of using drones equipped with ethylene sensors to assess apple maturity in an orchard. By modelling ethylene dispersion from multiple adjacent trees (Fig. 18), they assessed the optimal height for measurement. However, preliminary field experiments using a RW drone equipped with an ethylene AGS found that the proposed platform was unable to infer fruit maturity because of the sensor's high detection limit (500 ppb) with respect to the low concentrations of ethylene released (2 ppb according to the simulation).


Fig. 18. Simulated dispersion of ethylene vapors from climacteric fruits hanging from adjacent trees (Valente et al., 2019). Each tree is loaded with 20 kg of fruit and releases on average 100 ppb/s of ethylene. The maximum concentration (150 ppb) is found near the ground due to downwash of the RW drone.

## 6. Current limitations and future perspectives

In the last decade, drone-based chemical monitoring systems have emerged as an alternative or complementary technique to traditional ground-based detectors and manned aircraft in a myriad of applications ranging from volcanic plume analysis to methane leak detection in oil and gas industry. In this paper, we provide an exhaustive review of the potential applications of small drones fitted with in-situ or remote sensing gas detectors, explain in detail the various chemical-sensing technologies available, and describe the algorithmic solutions proposed to address tasks such as gas concentration mapping, source localization/identification, and flux quantification. While there is clearly great potential for drones in chemical sensing applications, it is also clear that this is still a very young field, and most work is still in the proof-of-concept stage, and needs further refinement and validation.

There are several barriers to progress in the acceptance/standardization of drone-based measurements. First, current microdrones still have limited operational capacity in terms of endurance, autonomy, and flight range. Short flying times (typically 15–20 min) make these systems unsuitable for large-scale screening in settings with low infrastructure density. Obstacle detection and avoidance is still not feasible in realistic scenarios, which requires a remote pilot to navigate those environments. Autonomous navigation is not envisioned in the short term, not only because of technical limitations, but also due to regulatory constraints. In most countries, drones can only be operated under certain conditions, such as in daylight, maintaining a visual line of sight (VLOS) between the operator and the drone, and a maximum altitude of 120 m and a safety distance from buildings and people. In certain applications, such as monitoring large industrial facilities, sniffer drones will need to have good maneuverability while also being able to cover large distances efficiently. The need for endurance and good maneuverability may be met by using RW drones with high-performance lithium polymer batteries (Hu et al., 2016), by using FW platforms with VTOL capability (Kalpa Gunarathna and Munasinghe, 2018) or by deploying multiple collaborating drones (He et al., 2019).

Second, the limited payload capacity of current microdrones prevents the use of heavy reference instrumentation on board, which often results in lower quality data. It is true that some high-end lightweight optical analyzers can be mounted on board, however they are currently only available for methane detection. While it may be acceptable in some scenarios to tether the drone to a ground-based instrument via a long sampling line, tethered tubing has significant practical disadvantages, such as risk of snaring on surface objects, contamination, sampling lag, and limited sampling range. Clearly, it is important to prioritise efforts to miniaturize high-precision analyzers and extend the range of gases they can detect, and improve the sensitivity, selectivity and response time of low-cost chemical sensors. In this line, a miniaturized mass spectrometer (MMS) and a miniaturized FTIR spectrometer were recently developed for use with small drones, allowing detailed composition analysis of volcanic plumes (Diaz et al., 2015) and simultaneous mapping of several compounds in an outdoor field (Rutkauskas et al., 2019), respectively. This represents a significant advance in the state of the art of drone-based gas measurements, i.e. using a laboratory-grade instrument on board of a small drone. Alternatively, combining signals from multiple gas sensors using pattern recognition algorithms is a promising way of increasing the selectivity of low-cost sensing technologies. The utility of e-noses for environmental monitoring applications has been already demonstrated in fixed installations (Bax et al., 2020), mobile robots (Palacín et al., 2019), and is currently being tested on drones (DAM-IBEC, 2019). Multivariable gas sensors, which consist of a sensing material with multi-response mechanisms to different gases, could offer a more compact form factor than e-noses, and better long-term stability of the sensor's output (Potyrailo, 2016).

Third, the downwash generated by the propellers of RW drones can reduce the quality of measured data. Moreover, the propellers produce considerable noise, which may hinder the social acceptance of using these drones in cities. Drone miniaturization, e.g. nano-drones, may reduce environmental and noise disturbance, and enable gas sensing operations inside buildings (Burgués et al., 2019a). However, as their physical size decreases, conventional motors become less efficient, and other required actuators become difficult to manufacture, creating a need for alternative methods of actuation for vehicles below a few grams. Inspired by nature, flapping-wing propulsion is a very efficient means of locomotion, and has the further advantage of minimal disturbance to surrounding air (Platzer et al., 2008). Under preliminary conditions, drone researchers have been able to reproduce natural flight in robotic insects such as the RoboBee (Wood et al., 2013) and the four-winged DelFly (De Croon et al., 2012), and in bird-sized drones such as the SmartBird (Mackenzie, 2012) or Nano Hummingbird (Keennon et al., 2012). A recent study described the hardware-software architecture of a flapping wing drone equipped with environmental sensors (Jatsun et al., 2018). These advances in the miniaturization of flying robots, and improvements in the performance of low-cost chemical sensors may drive a paradigm change in the field of environmental sensing using small drones. The original approach of using a large and heavy drone equipped with complex bulky instrumentation could likely be replaced by the use of swarms of insect-like collaborating drones equipped with very small gas sensors.

**Author contributions**

Conceptualization, J.B.; methodology, J.B.; investigation, J.B.; resources, S.M.; writing—original draft preparation, J.B.; writing—review and editing, J.B. and S.M.; visualization, J.B.; supervision, S.M.

**Funding**

This research has received funding from the ATTRACT project funded by the European Commission under Grant Agreement 777222, and by Spanish Ministerio de Asuntos Económicos y Transformación Digital (MINECO) under grant number BES-2015-071698 (Severo-Ochoa).

**Declaration of competing interest**

The authors declare that they have no known competing financial interests or personal relationships that could have appeared to influence the work reported in this paper.

**Acknowledgments**

CERCA Programme/Generalitat de Catalunya. The Signal and Information Processing for Sensor Systems group is a consolidated Grup de Recerca de la Generalitat de Catalunya and has support from the Departament d'Universitats, Recerca i Societat de la Informació de la Generalitat de Catalunya (expedient 2014-SGR-1445).

**References**

Aatamila, M., Verkasalo, P.K., Korhonen, M.J., Viluksela, M.K., Pasanen, K., Tiittanen, P., Nevalainen, A., 2010. Odor annoyance near waste treatment centers: a populationbased study in Finland. J. Air Waste Manage. Assoc. 60, 412–418.

Ability, A., 2019. ABB helps improve safety and profitability of oil and gas pipelines with drone-based gas leak detection [WWW document]. URL. https://new.abb.com/news/detail/17620/abb-helps-improve-safety-and-profitability-of-oil-and-gas-pipelines-with-drone-based-gas-leak-detection (accessed 4.30.20).

Allen, G., Hollingsworth, P., Kabbabe, K., Pitt, J.R., Mead, M.I., Illingworth, S., Roberts, G., Bourn, M., Shallcross, D.E., Percival, C.J., 2018. The development and trial of an unmanned aerial system for the measurement of methane flux from landfill and greenhouse gas emission hotspots. Waste Manag. https://doi.org/10.1016/j.wasman.2017.12.024 .

Alvarado, M., Gonzalez, F., Fletcher, A., Doshi, A., 2015. Towards the development of a low cost airborne sensing system to monitor dust particles after blasting at open-pit mine sites. Sensors (Switzerland) 15, 19667–19687. https://doi.org/10.3390/s150819667.

Alvarado, M., Gonzalez, F., Erskine, P., Cliff, D., Heuff, D., 2017. A methodology to monitor airborne PM10 dust particles using a small unmanned aerial vehicle. Sensors 17, 343.

Alvear, O., Zema, N.R., Natalizio, E., Calafate, C.T., 2017. Using UAV-based systems to monitor air pollution in areas with poor accessibility. J. Adv. Transp. 2017.

Andersen, P.C., Williford, C.J., Birks, J.W., 2010. Miniature personal ozone monitor based on UV absorbance. Anal. Chem. 82, 7924–7928.

Asenov, M., Rutkauskas, M., Reid, D., Subr, K., Ramamoorthy, S., 2019. Active localization of gas leaks using fluid simulation. IEEE Robot. Autom. Lett. 4, 1776–1783.

Aurell, J., Gullett, B.K., 2013. Emission factors from aerial and ground measurements of field and laboratory forest burns in the southeastern US: PM2. 5, black and brown carbon, VOC, and PCDD/PCDF. Environ. Sci. Technol. 47, 8443–8452.

Badia, S.B. i, Bernardet, U., Guanella, A., Pyk, P., Verschure, P.F.M.J., 2007. A biologically based chemo-sensing uav for humanitarian demining. Int. J. Adv. Robot. Syst. 4, 21.

Bakkum, E.A., Duijm, N.J., 1997. Vapour Cloud Dispersion, Yellow Book. CPR E. CPR E, London, UK.

Barchyn, T.E., Hugenholtz, C.H., Myshak, S., Bauer, J., 2017. A UAV-based system for detecting natural gas leaks. J. Unmanned Veh. Syst 6, 18–30.

Barchyn, T.E., Hugenholtz, C.H., Fox, T.A., 2019. Plume detection modeling of a dronebased natural gas leak detection system. Elem Sci Anth 7.

Baron, R., Saffell, J., 2017. Amperometric gas sensors as a low cost emerging technology platform for air quality monitoring applications: a review. ACS sensors 2, 1553–1566.

Bax, C., Sironi, S., Capelli, L., 2020. How can odors be measured? An overview of methods and their applications. Atmosphere (Basel) 11, 92.

Baxter, R.A., Bush, D.H., 2014. Use of small unmanned aerial vehicles for air quality and meteorological measurements. National Ambient Air Monitoring Conference (Aug 11–14). Atlanta, GA, USA.

Borrego, C., Costa, A.M., Ginja, J., Amorim, M., Coutinho, M., Karatzas, K., Sioumis, T., Katsifarakis, N., Konstantinidis, K., De Vito, S., et al., 2016. Assessment of air quality microsensors versus reference methods: the EuNetAir joint exercise. Atmos. Environ. 147, 246–263.

Borrego, C., Ginja, J., Coutinho, M., Ribeiro, C., Karatzas, K., Sioumis, T., Katsifarakis, N., Konstantinidis, K., De Vito, S., Esposito, E., et al., 2018. Assessment of air quality microsensors versus reference methods: the EuNetAir joint exercise—part II. Atmos. Environ. 193, 127–142.

BPX-Energy, 2019. BP North Sea deploys Mars technology in world-first methane monitoring project [WWW document]. URL. https://www.bp.com/en/global/corporate/news-and-insights/press-releases/bp-north-sea-deploys-mars-technology-in-worldfirst-methane-monitoring-project.html (accessed 3.31.20).

Brady, J.M., Stokes, M.D., Bonnardel, J., Bertram, T.H., 2016. Characterization of a quadrotor unmanned aircraft system for aerosol-particle-concentration measurements. Environ. Sci. Technol. 50, 1376–1383.

Brinkmann, T., Both, R., Scalet, B.M., Roudier, S., Sancho, L.D., 2018. JRC reference report on monitoring of emissions to air and water from IED installations; EUR 29261 EN. Eur. IPPC Bur. Eur. Comm. Jt. Res. Cent. https://doi.org/10.2760/344197.

Brosy, C., Krampf, K., Zeeman, M., Wolf, B., Junkermann, W., Schäfer, K., Emeis, S., Kunstmann, H., 2017. Simultaneous multicopter-based air sampling and sensing of meteorological variables. Atmos. Meas. Tech 10, 2773–2784. https://doi.org/10.5194/amt10-2773-2017.

Bui, X.-N., Lee, C., Nguyen, Q.L., Adeel, A., Cao, X.C., Nguyen, V.N., Le, V.C., Nguyen, H., Le, Q.T., Duong, T.H., et al., 2019. Use of unmanned aerial vehicles for 3D topographic mapping and monitoring the air quality of open-pit mines. Inżynieria Miner 21.

Burgués, J., Marco, S., 2018a. Multivariate estimation of the limit of detection by orthogonal partial least squares in temperature-modulated MOX sensors. Anal. Chim. Acta 1019, 49–64. https://doi.org/10.1016/j.aca.2018.03.005.

Burgués, J., Marco, S., 2018b. Low power operation of temperature-modulated metal oxide semiconductor gas sensors. Sensors (Switzerland) 18. https://doi.org/10.3390/s18020339.

Burgués, J., Marco, S., 2019. Wind-independent estimation of gas source distance from transient features of metal oxide sensor signals. IEEE Access 7, 140460–140469.

Burgués, J., Marco, S., 2020. Feature extraction for transient chemical sensor signals in response to turbulent plumes: application to chemical source distance prediction. Sensors Actuators B Chem. 128235.

Burgués, J., Jimenez-Soto, J.M., Marco, S., 2018. Estimation of the limit of detection in semiconductor gas sensors through linearized calibration models. Anal. Chim. Acta 1013, 13–25. https://doi.org/10.1016/j.aca.2018.01.062.

Burgués, J., Hernández, V., Lilienthal, A.J., Marco, S., 2019a. Smelling nano aerial vehicle for gas source localization and mapping. Sensors 19, 478.

Burgués, J., Valdez, L.F., Marco, S., 2019b. High-bandwidth e-nose for rapid tracking of turbulent plumes. 2019 ISOCS/IEEE International Symposium on Olfaction and Electronic Nose (ISOEN), pp. 1–3.

Burgués, J., Hernández, V., Lilienthal, A.J., Marco, S., 2020. Gas distribution mapping and source localization using a 3D grid of metal oxide semiconductor sensors. Sensors Actuators B Chem. 304, 127309.

Carrozzo, M., De Vito, S., Esposito, E., Salvato, M., Formisano, F., Massera, E., Di Francia, G., Veneri, P.D., Iadaresta, M., Mennella, A., 2018. UAV intelligent chemical multisensor payload for networked and impromptu gas monitoring tasks. 2018 5th IEEE International Workshop on Metrology for AeroSpace (MetroAeroSpace), Rome, Italy, 20–22 June, pp. 112–116.

Chatzidiakou, L., Krause, A., Popoola, O.A.M., Di Antonio, A., Kellaway, M., Han, Y., Squires, F.A., Wang, T., Zhang, H., Wang, Q., et al., 2019. Characterising low-cost sensors in highly portable platforms to quantify personal exposure in diverse environments. Atmos. Meas. Tech. 12, 4643.

Chen, X. xing, Huang, J., 2019. Odor source localization algorithms on mobile robots: a review and future outlook. Robot. Auton. Syst. 112, 123–136. https://doi.org/10.1016/j.robot.2018.11.014.

Chen, Z., Lu, C., 2005. Humidity sensors: a review of materials and mechanisms. Sens. Lett. 3, 274–295. https://doi.org/10.1166/sl.2005.045.

Collier-Oxandale, A., Feenstra, B., Papapostolou, V., Zhang, H., Kuang, M., Der Boghossian, B., Polidori, A., 2020. Field and laboratory performance evaluations of 28 gas-phase air quality sensors by the AQ-SPEC program. Atmos. Environ. 220, 117092.
ConocoPhillips, 2019. Testing drone technology to detect and quantify emissions [WWW

document]. URL. http://www.conocophillips.com/sustainability/sustainability-news/story/testing-drone-technology-to-detect-and-quantify-emissions/.

Crazzolara, C., Ebner, M., Platis, A., Miranda, T., Bange, J., Junginger, A., 2019. A new multicopter-based unmanned aerial system for pollen and spores collection in the atmospheric boundary layer. Atmos. Meas. Tech. 12, 1581–1598.

Daelman, M.R.J., van Voorthuizen, E.M., Van Dongen, L., Volcke, E.I.P., Van Loosdrecht, M.C.M., 2013. Methane and nitrous oxide emissions from municipal wastewater treatment—results from a long-term study. Water Sci. Technol. 67, 2350–2355.
DAM-IBEC, 2019. Drone-based environmental odour monitoring (SNIFFDRONE) [WWW document]. URL. https://attract-eu.com/selected-projects/sniffdrone-drone-basedenvironmental-odor-monitoring/ (accessed 11.18.19).

Danzer, K., Currie, L.A., 1998. Guidelines for calibration in analytical chemistry. Part I. Fundamentals and single component calibration (IUPAC recommendations 1998). Pure Appl. Chem. 70, 993–1014.

De Croon, G.C.H.E., Groen, M.A., De Wagter, C., Remes, B., Ruijsink, R., van Oudheusden, B.W., 2012. Design, aerodynamics and autonomy of the DelFly. Bioinspir. Biomim. 7, 25003.
de Man, I., 2018. Evaluation of an NO2 sensor mounted to a UAV for measuring air pollution [WWW document]. URL. http://edepot.wur.nl/470115 (accessed 9.29.20).

Diaz, J.A., Pieri, D., Wright, K., Sorensen, P., Kline-Shoder, R., Arkin, C.R., Fladeland, M., Bland, G., Buongiorno, M.F., Ramirez, C., et al., 2015. Unmanned aerial mass spectrometer systems for in-situ volcanic plume analysis. J. Am. Soc. Mass Spectrom. 26, 292–304.

Dinh, T.-V., Choi, I.-Y., Son, Y.-S., Kim, J.-C., 2016. A review on non-dispersive infrared gas sensors: improvement of sensor detection limit and interference correction. Sensors Actuators B Chem. 231, 529–538.

Emran, B.J., Tannant, D.D., Najjaran, H., 2017. Low-altitude aerial methane concentration mapping. Remote Sens. 9, 823. https://doi.org/10.3390/rs9080823.

Eu, K.S., Yap, K.M., 2018. Chemical plume tracing: a three-dimensional technique for quadrotors by considering the altitude control of the robot in the casting stage. Int. J. Adv. Robot. Syst. 15. https://doi.org/10.1177/1729881418755877.

Eu, K.S., Yap, K.M., Tee, T.H., 2014. An airflow analysis study of quadrotor based flying sniffer robot. Adv. Dev. Ind. Appl. Mech. 627. https://doi.org/10.4028/www.scientific.net/AMM.627.246.

Explicit-ApS, 2017. Airborne monitoring of sulphur emissions from ships in Danish waters [WWW document]. URL. https://www2.mst.dk/Udgiv/publications/2018/04/978-87-93710-00-9.pdf (accessed 10.9.19).

Eyring, V., Isaksen, I.S.A., Berntsen, T., Collins, W.J., Corbett, J.J., Endresen, O., Grainger, R.G., Moldanova, J., Schlager, H., Stevenson, D.S., 2010. Transport impacts on atmosphere and climate: shipping. Atmos. Environ. 44, 4735–4771.

Falabella, A.D., Wallin, D.O., Lund, J.A., 2018. Application of a customizable sensor platform to detection of atmospheric gases by UAS. 2018 International Conference on Unmanned Aircraft Systems (ICUAS), June 12–15. Dallas, TX, USA, pp. 883–890.

Farrell, J.A., Murlis, J., Long, X., Li, W., Cardé, R.T., 2002. Filament-based atmospheric dispersion model to achieve short time-scale structure of odor plumes. Environ. Fluid Mech. 2, 143–169. https://doi.org/10.1023/A:1016283702837.

Farrell, J.A., Pang, S., Li, W., 2003. Plume mapping via hidden Markov methods. IEEE Trans. Syst. Man, Cybern. Part B Cybern 33, 850–863. https://doi.org/10.1109/TSMCB.2003.810873.

Fine, G.F., Cavanagh, L.M., Afonja, A., Binions, R., 2010. Metal oxide semi-conductor gas sensors in environmental monitoring. Sensors 10, 5469–5502.

Fonollosa, J., Fernández, L., Gutiérrez-Gálvez, A., Huerta, R., Marco, S., 2016. Calibration transfer and drift counteraction in chemical sensor arrays using direct standardization. Sensors Actuators B Chem. 236, 1044–1053. https://doi.org/10.1016/j.snb.2016.05.089.

Fonollosa, J., Solórzano, A., Marco, S., 2018. Chemical sensor systems and associated algorithms for fire detection: a review. Sensors (Switzerland) 18. https://doi.org/10.3390/s18020553.

Frederiksen, M.H., Knudsen, M.P., 2018. Drones for offshore and maritime missions: opportunities and barriers [WWW document]. URL. SDU Cent. Integr. Innov. Manag https://uasdenmark.dk/wp-content/uploads/2019/06/Drones-for-offshoreand-maritime-missions_SDU_Spring-2018.pdf (accessed 9.29.19).

Gardner, J.W., Bartlett, P.N., 1999. Electronic noses. Principles and applications. Meas. Sci. Technol. 11, 1087.

Golston, L.M., Tao, L., Brosy, C., Schäfer, K., Wolf, B., McSpiritt, J., Buchholz, B., Caulton, D.R., Pan, D., Zondlo, M.A., et al., 2017. Lightweight mid-infrared methane sensor for unmanned aerial systems. Appl. Phys. B Lasers Opt. 123, 170.

Golston, L.M., Aubut, N.F., Frish, M.B., Yang, S., Talbot, R.W., Gretencord, C., McSpiritt, J., Zondlo, M.A., 2018a. Natural gas fugitive leak detection using an unmanned aerial vehicle: localization and quantification of emission rate. Atmosphere (Basel) 9. https://doi.org/10.3390/atmos9090333.

Golston, L.M., Aubut, N.F., Frish, M.B., Yang, S., Talbot, R.W., Gretencord, C., McSpiritt, J., Zondlo, M.A., 2018b. Natural gas fugitive leak detection using an unmanned aerial vehicle: localization and quantification of emission rate. Atmosphere (Basel) 9, 333. https://doi.org/10.3390/atmos9090333.

Goodwin, T., Carr, R., Mitra, A.K., Selmic, R.R., 2009. Coupled sensor/platform control design for low-level chemical detection with position-adaptive micro-UAVs. Evolutionary and Bio-inspired Computation: Theory and Applications III, p. 734710.

Gramm, A., Schütze, A., 2003. High performance solvent vapor identification with a two sensor array using temperature cycling and pattern classification. Sensors Actuators B Chem. 95, 58–65.

Greatwood, C., Richardson, T., Freer, J., Thomas, R., MacKenzie, A., Brownlow, R., Lowry, D., Fisher, R., Nisbet, E., 2017. Atmospheric sampling on Ascension island using multirotor UAVs. Sensors 17, 1189.

Gründler, P., 2007. Chemical Sensors: An Introduction for Scientists and Engineers. Springer Science & Business Media.

Gutierrez-Osuna, R., Gutierrez-Galvez, A., Powar, N., 2003. Transient response analysis for temperature-modulated chemoresistors. Sensors Actuators B Chem. 93, 57–66.
Hards, V.L., 2005. Volcanic contributions to the global carbon cycle [WWW document]. URL. https://www.bgs.ac.uk/downloads/start.cfm?id=432 (accessed 10.10.19).

He, X., Steiner, J.A., Bourne, J.R., Leang, K.K., 2019. Gaussian-based kernel for multi-agent aerial chemical-plume mapping. ASME 2019 Dynamic Systems and Control Conference (October 8–11) (Park City, Utah, USA).

Hernandez Bennetts, V., Lilienthal, A.J., Neumann, P.P., Trincavelli, M., 2012a. Mobile Robots for Localizing Gas Emission Sources on Landfill Sites: Is Bio-inspiration the Way to Go? vol. 4, p. 20. https://doi.org/10.3389/fneng.2011.00020

Hernandez Bennetts, V., Lilienthal, A.J., Neumann, P.P., Trincavelli, M., 2012b. Mobile robots for localizing gas emission sources on landfill sites: is bio-inspiration the way to go? Front. Neuroeng. 4. https://doi.org/10.3389/fneng.2011.00020.

Hodgkinson, J., Tatam, R.P., 2013. Optical gas sensing: a review. Meas. Sci. Technol. https://doi.org/10.1088/0957-0233/24/1/012004.

Hollenbeck, D., Dahabra, M., Christensen, L.E., Chen, Y., 2019a. Data quality aware flight mission design for fugitive methane sniffing using fixed wing sUAS. In: IEEE (Ed.), 2019 International Conference on Unmanned Aircraft Systems (ICUAS). IEEE, Atlanta, GA, USA, pp. 813–818.

Hollenbeck, D., Oyama, M., Garcia, A., Chen, Y., 2019b. Pitch and roll effects of on-board wind measurements using sUAS. 2019 International Conference on Unmanned Aircraft Systems (ICUAS), pp. 1249–1254 Atlanta, GA, USA.

Hu, P., Chai, J., Duan, Y., Liu, Z., Cui, G., Chen, L., 2016. Progress in nitrile-based polymer electrolytes for high performance lithium batteries. J. Mater. Chem. A 4, 10070–10083.

Hugenholtz, C.H., Moorman, B.J., Riddell, K., Whitehead, K., 2012. Small unmanned aircraft systems for remote sensing and earth science research. EOS Trans. Am. Geophys. Union 93, 236.

Hunter, G.W., Akbar, S., Bhansali, S., Daniele, M., Erb, P.D., Johnson, K., Liu, C.-C., Miller, D., Oralkan, O., Hesketh, P.J., et al., 2020. Editors' choice—critical review—a critical review of solid state gas sensors. J. Electrochem. Soc. 167, 37570.

Hutchinson, M., Liu, C., Chen, W.-H., 2018. Information-based search for an atmospheric release using a mobile robot: algorithm and experiments. IEEE Trans. Control Syst. Technol. 27, 2388–2402.

Hutchinson, M., Liu, C., Chen, W.-H., 2019. Source term estimation of a hazardous airborne release using an unmanned aerial vehicle. J. F. Robot. 36, 797–817.

Ishida, H., 2009. Blimp robot for three-dimensional gas distribution mapping in indoor environment. AIP Conference Proceedings, pp. 61–64 https://doi.org/10.1063/1.3156627.

Jatsun, S.F., Korenevskiy, N.A., Efimov, S.V., Korovin, E.N., 2018. An automated system for monitoring the environment and assessing people's status in extreme situations using a flying robot. Biomed. Eng. (NY). 52, 287–290.

Jiao, W., Hagler, G., Williams, R., Sharpe, R., Brown, R., Garver, D., Judge, R., Caudill, M., Rickard, J., Davis, M., et al., 2016. Community Air Sensor Network (CAIRSENSE) project: evaluation of low-cost sensor performance in a suburban environment in the southeastern United States. Atmos. Meas. Tech. 9.

Kalpa Gunarathna, J., Munasinghe, R., 2018. Development of a quad-rotor fixed-wing hybrid unmanned aerial vehicle. 2018 Moratuwa Engineering Research Conference (MERCon), May 30–June 1, pp. 72–77 Moratuwa, Sri Lanka.

Kang, Z.-Q., Meng, Q.-H., Luo, B., Wang, J.-Y., Dai, X.-Y., Ma, S.-G., 2018. Experimental verification of an aerodynamic olfactory effect model for the simulation of gas-sensitive rotorcrafts. 2018 13th World Congress on Intelligent Control and Automation (WCICA), pp. 1652–1657.

Keennon, M., Klingebiel, K., Won, H., 2012. Development of the nano hummingbird: a tailless flapping wing micro air vehicle. 50th AIAA Aerospace Sciences Meeting Including the New Horizons Forum and Aerospace Exposition, p. 588.

Kersnovski, T., Gonzalez, F., Morton, K., 2017. A UAV system for autonomous target detection and gas sensing. 2017 IEEE Aerospace Conference (March 4th–11th), pp. 1–12 Big Sky, MT, USA.

Keys, R., 1981. Cubic convolution interpolation for digital image processing. IEEE Trans. Acoust. 29, 1153–1160.

Khan, A., Schaefer, D., Tao, L., Miller, D.J., Sun, K., Zondlo, M.A., Harrison, W.A., Roscoe, B., Lary, D.J., 2012a. Low power greenhouse gas sensors for unmanned aerial vehicles. Remote Sens. 4, 1355–1368. https://doi.org/10.3390/rs4051355.

Khan, M.A., Zondlo, M.A., Lary, D.J., 2012b. Open-path greenhouse gas sensor for UAV applications. Conf. Lasers Electro-Optics 2012, 1 JTh1L.6. https://doi.org/10.1364/CLEO_AT.2012.JTh1L.6.

Kiani, S., Minaei, S., Ghasemi-Varnamkhasti, M., 2016. Application of electronic nose systems for assessing quality of medicinal and aromatic plant products: a review. J. Appl. Res. Med. Aromat. Plants 3, 1–9.

Kitsukawa, S., Nakagawa, H., Fukuda, K., Asakura, S., Takahashi, S., Shigemori, T., 2000. The interference elimination for gas sensor by catalyst filters. Sensors Actuators B Chem. 65, 120–121.

Knorr, W., Jiang, L., Arneth, A., 2016. Climate, CO2 and human population impacts on global wildfire emissions. Biogeosciences 13.

Korotcenkov, G., Cho, B.K., 2013. Engineering approaches for the improvement of conductometric gas sensor parameters: part 1. Improvement of sensor sensitivity and selectivity (short survey). Sensors Actuators B Chem. 188, 709–728.

Korotcenkov, G., Cho, B.K., 2017. Metal oxide composites in conductometric gas sensors: achievements and challenges. Sensors Actuators B Chem. 244, 182–210.

Koval, A., Irigoyen, E., Koval, T., 2017. AR. Drone as a platform for measurements. 2017 IEEE 37th International Conference on Electronics and Nanotechnology (ELNANO), pp. 424–427.

Kowadlo, G., Russell, R.A., 2008. Robot odor localization: a taxonomy and survey. Int. J. Robot. Res. 27, 869–894. https://doi.org/10.1177/0278364908095118.

Koziar, Y., Levchuk, V., Koval, A., 2019. Quadrotor design for outdoor air quality monitoring. 2019 IEEE 39th International Conference on Electronics and Nanotechnology (ELNANO), pp. 736–739.

Krüll, W., Tobera, R., Willms, I., Essen, H., Von Wahl, N., 2012. Early forest fire detection and verification using optical smoke, gas and microwave sensors. Procedia Eng 45, 584–594. https://doi.org/10.1016/j.proeng.2012.08.208.

Kuantama, E., Tarca, R., Dzitac, S., Dzitac, I., Vesselenyi, T., Tarca, I., 2019. The design and experimental development of air scanning using a sniffer quadcopter. Sensors 19, 3849.

Kunz, M., Lavric, J.V., Gerbig, C., Tans, P., Neff, D., Hummelgård, C., Martin, H., Rödjegård, H., Wrenger, B., Heimann, M., 2018. COCAP: a carbon dioxide analyser for small unmanned aircraft systems. Atmos. Meas. Tech 11, 1833–1849.

Kunz, M., Lavric, J.V., Gasche, R., Gerbig, C., Grant, R.H., Koch, F.-T., Schumacher, M., Wolf, B., Zeeman, M., 2019. Surface flux estimates derived from UAS-based mole fraction measurements by means of a nocturnal boundary layer budget approach. Atmos. Meas. Tech. Discuss. 13, 1671–1692.

Lam, N.S.-N., 1983. Spatial interpolation methods: a review. Am. Cartogr. 10, 129–150.
Lee, A.P., Reedy, B.J., 1999. Temperature modulation in semiconductor gas sensing. Sensors Actuators B Chem. 60, 35–42. https://doi.org/10.1016/S0925-4005(99)00241-5.

Lega, M., Napoli, R.M.A., 2008. A new approach to solid waste landfills aerial monitoring. WIT Trans. Ecol. Environ. 109, 193–199. https://doi.org/10.2495/WM080211.

Letheren, B., Montes, G., Villa, T., Gonzalez, F., 2016. Design and flight testing of a bioinspired plume tracking algorithm for unmanned aerial vehicles. IEEE Aerospace Conference Proceedings https://doi.org/10.1109/AERO.2016.7500614.

Li, X.-B., Wang, D.-S., Lu, Q.-C., Peng, Z.-R., Lu, S.-J., Li, B., Li, C., 2017. Three-dimensional investigation of ozone pollution in the lower troposphere using an unmanned aerial vehicle platform. Environ. Pollut. 224, 107–116.

Licen, S., Di Gilio, A., Palmisani, J., Petraccone, S., de Gennaro, G., Barbieri, P., 2020. Pattern recognition and anomaly detection by self-organizing maps in a multi month E-nose survey at an industrial site. Sensors 20, 1887.

Lilienthal, A., Duckett, T., 2004. Building gas concentration gridmaps with a mobile robot. Robot. Auton. Syst. 48, 3–16. https://doi.org/10.1016/j.robot.2004.05.002.

Liu, E.J., Wood, K., Mason, E., Edmonds, M., Aiuppa, A., Giudice, G., Bitetto, M., Francofonte, V., Burrow, S., Richardson, T., et al., 2019. Dynamics of outgassing and plume transport revealed by proximal Unmanned Aerial System (UAS) measurements at Volcán

Villarrica, Chile. Geochem. Geophys. Geosyst. 20, 730–750.
Lou, X.F., Nair, J., 2009. The impact of landfilling and composting on greenhouse gas emissions—a review. Bioresour. Technol. 100, 3792–3798.

Loutfi, A., Coradeschi, S., Mani, G.K., Shankar, P., Rayappan, J.B.B., 2015. Electronic noses for food quality: a review. J. Food Eng. 144, 103–111. https://doi.org/10.1016/j.jfoodeng.2014.07.019.

Luo, B., Meng, Q.H., Wang, J.Y., Sun, B., Wang, Y., 2015. Three-dimensional gas distribution mapping with a micro-drone. Chinese Control Conf. (CCC), Hangzhou, China, 28–30 July 2015-Septe, pp. 6011–6015 https://doi.org/10.1109/ChiCC.2015.7260580.

Luo, B., Meng, Q.H., Wang, J.Y., Ma, S.G., 2016. Simulate the aerodynamic olfactory effects of gas-sensitive UAVs: a numerical model and its parallel implementation. Adv. Eng. Softw. 102, 123–133. https://doi.org/10.1016/j.advengsoft.2016.10.001.

Luo, B., Meng, Q.H., Wang, J.Y., Zeng, M., 2017. A flying odor compass to autonomously locate the gas source. IEEE Trans. Instrum. Meas. 67, 137–149. https://doi.org/10.1109/TIM.2017.2759378.

Mackenzie, D., 2012. A flapping of wings [WWW document]. Science 335 (6075), 1430–1433. https://doi.org/10.1126/science.335.6075.1430 URL. https://science.sciencemag.org/content/335/6075/1430 (accessed 11.29.19).

Mafra-Neto, A., Cardé, R.T., 1994. Fine-scale structure of pheromone plumes modulates upwind orientation of flying moths. Nature 369, 142.

Malaver Rojas, J.A., Gonzalez, L.F., Motta, N., Villa, T.F., Etse, V.K., Puig, E., 2015. Design and flight testing of an integrated solar powered UAV and WSN for greenhouse gas monitoring emissions in agricultural farms. 2015 IEEE/RSJ International Conference on Intelligent Robots and Systems, pp. 1–6.

Marco, S., Gutierrez-Galvez, A., 2012. Signal and data processing for machine olfaction and chemical sensing: a review. IEEE Sensors J. https://doi.org/10.1109/JSEN.2012.2192920.

Martin, C.R., Zeng, N., Karion, A., Dickerson, R.R., Ren, X., Turpie, B.N., Weber, K.J., 2017. Evaluation and environmental correction of ambient CO2 measurements from a low-cost NDIR sensor. Atmos. Meas. Tech 10.

Martinez, D., Burgués, J., Marco, S., 2019. Fast measurements with MOX sensors: a leastsquares approach to blind deconvolution. Sensors 19, 4029.

Martinez, B., Miller, T.W., Yalin, A.P., 2020. Cavity ring-down methane sensor for small unmanned aerial systems. Sensors 20, 454.

McGonigle, A.J.S., Aiuppa, A., Giudice, G., Tamburello, G., Hodson, A.J., Gurrieri, S., 2008. Unmanned aerial vehicle measurements of volcanic carbon dioxide fluxes. Geophys. Res. Lett. 35. https://doi.org/10.1029/2007GL032508.

McKinney, K.A., Wang, D., Ye, J., de Fouchier, J.-B., Guimarães, P.C., Batista, C.E., Souza, R.A.F., Alves, E.G., Gu, D., Guenther, A.B., et al., 2019. A sampler for atmospheric volatile organic compounds by copter unmanned aerial vehicles. Atmos. Meas. Tech. 12, 3123–3135.
McRae, T.G., Kulp, T.J., 1993. Backscatter absorption gas imaging: a new technique for gas visualization. Appl. Opt. 32, 4037–4050.

Monroy, J.G., Gonźalez-Jiḿenez, J., Blanco, J.L., 2012. Overcoming the slow recovery of MOX gas sensors through a system modeling approach. Sensors (Switzerland) 12, 13664–13680. https://doi.org/10.3390/s121013664.

Mori, T., Hashimoto, T., Terada, A., Yoshimoto, M., Kazahaya, R., Shinohara, H., Tanaka, R., 2016. Volcanic plume measurements using a UAV for the 2014 Mt. Ontake eruption the phreatic eruption of Mt. Ontake Volcano in 2014 5. Volcanology. Earth, Planets Sp, 68 https://doi.org/10.1186/s40623-016-0418-0.

Muscato, G., Bonaccorso, F., Cantelli, L., Longo, D., Melita, C.D., 2012. Volcanic environments: robots for exploration and measurement. IEEE Robot. Autom. Mag. 19, 40–49.
Nassif, N., 2012. A robust CO2-based demand-controlled ventilation control strategy for multi-zone HVAC systems. Energy Build 45, 72–81.

Nathan, B.J., Golston, L.M., O'Brien, A.S., Ross, K., Harrison, W.A., Tao, L., Lary, D.J., Johnson, D.R., Covington, A.N., Clark, N.N., et al., 2015. Near-field characterization of methane emission variability from a compressor station using a model aircraft. Environ. Sci. Technol. 49, 7896–7903.

Neumann, P.P., Asadi, S., Lilienthal, A.J., Bartholmai, M., Schiller, J.H., 2012. Autonomous gas-sensitive microdrone: wind vector estimation and gas distribution mapping. IEEE Robot. Autom. Mag. 19, 50–61. https://doi.org/10.1109/MRA.2012.2184671.

Neumann, P.P., Kohlhoff, H., Hüllmann, D., Krentel, D., Kluge, M., Dzierliński, M., Lilienthal, A.J., Bartholmai, M., 2019. Aerial-based gas tomography—from single beams to complex gas distributions. Eur. J. Remote Sens 1–15.

Oberle, F.K.J., Gibbs, A.E., Richmond, B.M., Erikson, L.H., Waldrop, M.P., Swarzenski, P.W., 2019. Towards determining spatial methane distribution on Arctic permafrost bluffs with an unmanned aerial system. SN Appl. Sci. 1, 236.

Oluwoye, I., Dlugogorski, B.Z., Gore, J., Oskierski, H.C., Altarawneh, M., 2017. Atmospheric emission of NOx from mining explosives: a critical review. Atmos. Environ. 167, 81–96.
Pajares, G., 2015. Overview and current status of remote sensing applications based on unmanned aerial vehicles (UAVs). Photogramm. Eng. Remote. Sens. 81, 281–330. https://doi.org/10.14358/PERS.81.4.281.

Palacín, J., Martínez, D., Clotet, E., Pallejà, T., Burgués, J., Fonollosa, J., Pardo, A., Marco, S., 2019. Application of an array of metal-oxide semiconductor gas sensors in an assistant personal robot for early gas leak detection. Sensors 19, 1957. https://doi.org/10.3390/s19091957.

Palmiotto, M., Fattore, E., Paiano, V., Celeste, G., Colombo, A., Davoli, E., 2014. Influence of a municipal solid waste landfill in the surrounding environment: toxicological risk and odor nuisance effects. Environ. Int. 68, 16–24.

Palomaki, R.T., Rose, N.T., van den Bossche, M., Sherman, T.J., De Wekker, S.F.J., 2017. Wind estimation in the lower atmosphere using multirotor aircraft. J. Atmos. Ocean. Technol. 34, 1183–1191.

Patel, P., 2017. Monitoring methane. ACS Cent. Sci. 3, 679–682. https://doi.org/10.1021/acscentsci.7b00292.

Piedrahita, R., Xiang, Y., Masson, N., Ortega, J., Collier, A., Jiang, Y., Li, K., Dick, R.P., Lv, Q., Hannigan, M., et al., 2014. The next generation of low-cost personal air quality sensors for quantitative exposure monitoring. Atmos. Meas. Tech. 7, 3325.

Pieri, D., Diaz, J.A., Bland, G., Fladeland, M., Madrigal, Y., Corrales, E., Alegria, O., Alan, A., Realmuto, V., Miles, T., et al., 2013. In situ observations and sampling of volcanic emissions with NASA and UCR unmanned aircraft, including a case study at Turrialba Volcano, Costa Rica. Geol. Soc. Lond. Spec. Publ. 380, 321–352.

Platzer, M.F., Jones, K.D., Young, J., S. Lai, J.C., 2008. Flapping wing aerodynamics: progress and challenges. AIAA J. 46, 2136–2149.

Pobkrut, T., Eamsa-Ard, T., Kerdcharoen, T., 2016. Sensor drone for aerial odor mapping for agriculture and security services. 2016 13th Int. Conf. Electr. Eng. Comput. Telecommun. Inf. Technol. ECTI-CON 2016, Chiang Mai, Thailand, 28 June–1 July, pp. 1–5 https://doi.org/10.1109/ECTICon.2016.7561340.

Pomareda, V., Magrans, R., Jiménez-Soto, J.M., Martínez, D., Tresánchez, M., Burgués, J., Palacín, J., Marco, S., 2017. Chemical source localization fusing concentration information in the presence of chemical background noise. Sensors (Switzerland) 17. https://doi.org/10.3390/s17040904.

Popa, D., Udrea, F., Popa, D., Udrea, F., 2019. Towards integrated mid-infrared gas sensors. Sensors 19, 2076. https://doi.org/10.3390/s19092076.

Poppa, F., Zimmer, U., Feitz, A., Berko, H., 2013. Development of a carbon dioxide monitoring rotorcraft unmanned aerial vehicle. Robotics: Science and Systems (RSS) Workshop on Robotics for Environmental Monitoring (WREM), pp. 24–28.

Potyrailo, R.A., 2016. Multivariable sensors for ubiquitous monitoring of gases in the era of internet of things and industrial internet. Chem. Rev. 116, 11877–11923.

Price, P.N., Fischer, M.L., Gadgil, A.J., Sextro, R.G., 2001. An algorithm for real-time tomography of gas concentrations, using prior information about spatial derivatives. Atmos. Environ. 35, 2827–2835.

Prudden, S., Fisher, A., Mohamed, A., Watkins, S., 2016. A flying anemometer quadrotor: part 1. Proc International Micro Air Vehicle Conference (IMAV 2016).

Qiu, S., Chen, B., Wang, R., Zhu, Z., Wang, Y., Qiu, X., 2017. Estimating contaminant source in chemical industry park using UAV-based monitoring platform, artificial neural network and atmospheric dispersion simulation. RSC Adv. 7, 39726–39738.

RAE-Systems, 2014. The PID handbook: theory and applications of direct-reading photoionization detectors. [WWW Document]. URL. https://www.raesystems.com/sites/default/files/content/resources/pid_handbook_1002-02.pdf (accessed 12.12.19).

Rahbar, F., Marjovi, A., Kibleur, P., Martinoli, A., 2017. A 3-D bio-inspired odor source localization and its validation in realistic environmental conditions. 2017 IEEE/RSJ International Conference on Intelligent Robots and Systems (IROS), pp. 3983–3989.

Ravikumar, A.P., Wang, J., Brandt, A.R., 2017. Are optical gas imaging technologies effective for methane leak detection? Environ. Sci. Technol. 51, 718–724. https://doi.org/10.1021/acs.est.6b03906.

Ravikumar, A.P., Wang, J., McGuire, M., Bell, C.S., Zimmerle, D., Brandt, A.R., 2018. "Good versus good enough?" Empirical tests of methane leak detection sensitivity of a commercial infrared camera. Environ. Sci. Technol. 52, 2368–2374.

Ravikumar, A.P., Sreedhara, S., Wang, J., Englander, J., Roda-Stuart, D., Bell, C., Zimmerle, D., Lyon, D., Mogstad, I., Ratner, B., et al., 2019. Single-blind inter-comparison of methane detection technologies–results from the Stanford/EDF mobile monitoring challenge. Elem Sci Anth 7.

Rehfuess, E., 2006. Fuel for life: household energy and health [WWW document]. URL. World Heal. Organ https://www.who.int/airpollution/publications/fuelforlife.pdf (accessed 10.20.19).

Rezende, G.C., Le Calvé, S., Brandner, J.J., Newport, D., 2019. Micro photoionization detectors. Sensors Actuators B Chem. 287, 86–94.

Robock, A., 2000. Volcanic eruptions and climate. Rev. Geophys. 38, 191–219.

Roldán, J.J., Joossen, G., Sanz, D., del Cerro, J., Barrientos, A., 2015. Mini-UAV based sensory system for measuring environmental variables in greenhouses. Sensors (Switzerland) 15, 3334–3350. https://doi.org/10.3390/s150203334.

Roldán, J., Garcia-Aunon, P., Garzón, M., de León, J., del Cerro, J., Barrientos, A., 2016. Heterogeneous multi-robot system for mapping environmental variables of greenhouses. Sensors 16, 1018.

Romain, A.C., Nicolas, J., 2010. Long term stability of metal oxide-based gas sensors for enose environmental applications: an overview. Sensors Actuators B Chem. 146, 502–506. https://doi.org/10.1016/j.snb.2009.12.027.

Rossi, M., Brunelli, D., Adami, A., Lorenzelli, L., Menna, F., Remondino, F., 2014. Gas-drone: portable gas sensing system on UAVs for gas leakage localization. Proceedings of IEEE Sensors, pp. 1431–1434 https://doi.org/10.1109/ICSENS.2014.6985282.

Ruddick, J., Marjovi, A., Rahbar, F., Martinoli, A., 2018. Design and performance evaluation of an infotaxis-based three-dimensional algorithm for odor source localization. 2018 IEEE/RSJ International Conference on Intelligent Robots and Systems (IROS), pp. 1413–1420.

Rüdiger, J., Tirpitz, J.L., Maarten De Moor, J., Bobrowski, N., Gutmann, A., Liuzzo, M., Ibarra, M., Hoffmann, T., 2018. Implementation of electrochemical, optical and denuderbased sensors and sampling techniques on UAV for volcanic gas measurements: examples from Masaya, Turrialba and Stromboli volcanoes. Atmos. Meas. Tech 11, 2441–2457. https://doi.org/10.5194/amt-11-2441-2018.

Rutkauskas, M., Asenov, M., Ramamoorthy, S., Reid, D.T., 2019. Autonomous multi-species environmental gas sensing using drone-based Fourier-transform infrared spectroscopy. Opt. Express 27, 9578–9587.

Sanchez-Cuevas, P., Heredia, G., Ollero, A., 2017. Characterization of the aerodynamic ground effect and its influence in multirotor control. Int. J. Aerosp. Eng. 2017.
Scentroid, 2018. EU police using Scentroid DR1000 flying lab to combat smog [WWW document]. URL. http://scentroid.com/police-using-scentroid-dr1000-flying-lab-tocombat-smog/ (accessed 6.4.18).

Schuur, E.A.G., McGuire, A.D., Schädel, C., Grosse, G., Harden, J.W., Hayes, D.J., Hugelius, G., Koven, C.D., Kuhry, P., Lawrence, D.M., et al., 2015. Climate change and the permafrost carbon feedback. Nature 520, 171–179.

Schuyler, T., Guzman, M., 2017. Unmanned aerial systems for monitoring trace tropospheric gases. Atmosphere (Basel) 8, 206.

Schuyler, T.J., Bailey, S.C.C., Guzman, M.I., 2019. Monitoring tropospheric gases with small unmanned aerial systems (sUAS) during the second CLOUDMAP flight campaign. Atmosphere (Basel) 10, 434.

Scire, J.S., Strimaitis, D.G., Yamartino, R.J., et al., 2000. A User's Guide for the CALPUFF Dispersion Model. vol. 521. Earth Tech, Inc, pp. 1–521.

Seiyama, T., 2013. Chemical Sensor Technology. vol. 2. Elsevier.

Shah, A., Allen, G., Pitt, J.R., Ricketts, H., Williams, P.I., Helmore, J., Finlayson, A., Robinson, R., Kabbabe, K., Hollingsworth, P., et al., 2019a. A near-field Gaussian plume inversion flux quantification method, applied to unmanned aerial vehicle sampling. Atmosphere (Basel) 10, 396.

Shah, A., Pitt, J., Kabbabe, K., Allen, G., 2019b. Suitability of a non-dispersive infrared methane sensor package for flux quantification using an unmanned aerial vehicle. Sensors 19, 4705.

Shigaki, S., Fikri, M., Kurabayashi, D., 2018. Design and experimental evaluation of an odor sensing method for a pocket-sized quadcopter. Sensors 18, 3720.

Shinohara, H., 2013. Composition of volcanic gases emitted during repeating Vulcanian eruption stage of Shinmoedake, Kirishima volcano, Japan. Earth, Planets Sp 65, 667–675. https://doi.org/10.5047/eps.2012.11.001.

Shukla, D., Komerath, N., 2018. Multirotor drone aerodynamic interaction investigation. Drones 2, 43.

Sibson, R., 1981. A brief description of natural neighbour interpolation. In: Barnett, V. (Ed.), Interpreting Multivariate Data. John Wiley & Sons, pp. 21–36.

Sjöholm, M., Angelou, N., Hansen, P., Hansen, K.H., Mikkelsen, T., Haga, S., Silgjerd, J.A., Starsmore, N., 2014. Two-dimensional rotorcraft downwash flow field measurements by lidar-based wind scanners with agile beam steering. J. Atmos. Ocean. Technol. 31, 930–937.

Smith, B., John, G., Stark, B., Christensen, L.E., Chen, Y., 2016. Applicability of unmanned aerial systems for leak detection. 2016 International Conference on Unmanned Aircraft Systems (ICUAS), pp. 1220–1227.

Smith, B.J., John, G., Christensen, L.E., Chen, Y., 2017. Fugitive methane leak detection using sUAS and miniature laser spectrometer payload: system, application and groundtruthing tests. 2017 International Conference on Unmanned Aircraft Systems (ICUAS), pp. 369–374.

Spinelle, L., Gerboles, M., Villani, M.G., Aleixandre, M., Bonavitacola, F., 2015. Field calibration of a cluster of low-cost available sensors for air quality monitoring. Part A: ozone and nitrogen dioxide. Sensors Actuators B Chem. 215, 249–257.

Spinelle, L., Gerboles, M., Villani, M.G., Aleixandre, M., Bonavitacola, F., 2017. Field calibration of a cluster of low-cost commercially available sensors for air quality monitoring. Part B: NO, CO and CO2. Sensors Actuators B Chem. 238, 706–715.

Stetter, J.R., Li, J., 2008. Amperometric gas sensors a review. Chem. Rev. 108, 352–366.

Stetter, J.R., Pan, L., 1994. Amperometric Carbon Monoxide Sensor Module for Residential Alarms.

Takei, Y., Kanazawa, Y., Hirasawa, K., Nanto, H., 2019. Development of 3D gas source localization using multi-copter with gas sensor array. 2019 IEEE International Symposium on Olfaction and Electronic Nose (ISOEN), pp. 1–4.

Tannant, D., Smith, K., Cahill, A., Hawthorne, I., Ford, O., Black, A., Beckie, R., 2018. Evaluation of a Drone and Laser-based Methane Sensor for Detection of Fugitive Methane Emissions. Submitt. to Br. Columbia Oil Gas Res. Innov. Soc.

Tittel, F.K., Bakhirkin, Y.A., Curl, R.F., Kosterev, A.A., McCurdy, M.R., So, S.G., Wysocki, G., 2008. Laser based chemical sensor technology: recent advances and applications. Advanced Environmental Monitoring. Springer, pp. 50–63.

Topali, D., Psaraftis, H.N., 2019. The enforcement of the global sulfur cap in maritime transport. Marit. Bus. Rev. 4, 199–216. https://doi.org/10.1108/MABR-12-2018-0050.

TOTAL Group, 2019. Integrating climate into our strategy [WWW document]. URL. https://www.total.com/sites/default/files/atoms/files/total_rapport_climat_2019_en.pdf#page=30 (accessed 3.29.20).

Tran, T.V., Dang, N.T., Chung, W.-Y., 2017. Battery-free smart-sensor system for real-time indoor air quality monitoring. Sensors Actuators B Chem. 248, 930–939.

Trincavelli, M., Bennetts, V.H., Lilienthal, A.J., 2012. A least squares approach for learning gas distribution maps from a set of integral gas concentration measurements obtained with a TDLAS sensor. Proc. IEEE Sensors https://doi.org/10.1109/ICSENS.2012.6411118.

Tuller, H.L., 2013. Materials for high temperature electrochemical applications: automotive sensors, catalysts and traps. Sensors Actuators B Chem. 187, 106–110.

United Nations Economic Commission for Europe (UNECE), 2008. Guidance to the protocol on pollutant release and transfer registers [WWW document]. URL. https://www.unece.org/env/pp/prtr.guidancedev.html (accessed 9.9.19).

United States Environmental Protection Agency (EPA), n.d. Leak detection and repair: a best practices guide [WWW document]. URL https://www.epa.gov/compliance/leak-detection-and-repair-best-practices-guide (accessed 7.10.19).

Valente, J., Almeida, R., Kooistra, L., 2019. A comprehensive study of the potential application of flying ethylene-sensitive sensors for ripeness detection in apple orchards. Sensors 19, 372.

Vergassola, M., Villermaux, E., Shraiman, B.I., 2007. "Infotaxis" as a strategy for searching without gradients. Nature 445, 406–409. https://doi.org/10.1038/nature05464.

Villa, T., Gonzalez, F., Miljievic, B., Ristovski, Z., Morawska, L., 2016. An overview of small unmanned aerial vehicles for air quality measurements: present applications and future prospectives. Sensors 16, 1072. https://doi.org/10.3390/s16071072.

Vincent, T.A., Gardner, J.W., 2016. A low cost MEMS based NDIR system for the monitoring of carbon dioxide in breath analysis at ppm levels. Sensors Actuators B Chem. 236, 954–964.

von Glasow, R., Bobrowski, N., Kern, C., 2009. The effects of volcanic eruptions on atmospheric chemistry. Chem. Geol. 263, 131–142.

Von Wahl, N., Heinen, S., Essen, H., Kruell, W., Tobera, R., Willms, I., 2010. An integrated approach for early forest fire detection and verification using optical smoke, gas and microwave sensors. WIT Trans. Ecol. Environ. 137, 97–106.

Wales, D.J., Grand, J., Ting, V.P., Burke, R.D., Edler, K.J., Bowen, C.R., Mintova, S., Burrows, A.D., 2015. Gas sensing using porous materials for automotive applications. Chem. Soc. Rev. 44, 4290–4321.

Wang, C., Yin, L., Zhang, L., Xiang, D., Gao, R., 2010. Metal oxide gas sensors: sensitivity and influencing factors. Sensors https://doi.org/10.3390/s100302088.

Wang, F., Jia, S., Wang, Y., Tang, Z., 2019. Recent developments in modulation spectroscopy for methane detection based on tunable diode laser. Appl. Sci. 9, 2816.

Watai, T., Machida, T., Ishizaki, N., Inoue, G., Watai, T., Machida, T., Ishizaki, N., Inoue, G., 2006. A lightweight observation system for atmospheric carbon dioxide concentration using a small unmanned aerial vehicle. J. Atmos. Ocean. Technol. 23, 700–710. https://doi.org/10.1175/JTECH1866.1.

Wei, P., Ning, Z., Ye, S., Sun, L., Yang, F., Wong, K.C., Westerdahl, D., Louie, P.K.K., 2018. Impact analysis of temperature and humidity conditions on electrochemical sensor response in ambient air quality monitoring. Sensors 18, 59.

Whitehead, K., 2018. Development of an innovative UAV-mounted system for the detection of fugitive methane emissions [WWW document]. URL. https://www.ptac.org/wp-content/uploads/2018/12/08.-Ken-Whitehead-1.pdf (accessed 10.10.19).

Whiticar, M.J., Christensen, L.E., Salas, C.J., Reece, P., 2018. GHGMap: novel approach for aerial measurements of greenhouse gas emissions, British Columbia. Geoscience BC Summary of Activities 2017: Energy, Geoscience BC, Report 2018-4, pp. 1–10.

Whiticar, M.J., Christensen, L.E., Salas, C.J., Reece, P., 2019. GHGMap: detection of fugitive methane leaks from natural gas pipelines, British Columbia and Alberta. Geoscience BC Summary of Activities 2018: Energy and Water, Geoscience BC, Report 2019-2, pp. 67–76.

Wivou, J., Udawatta, L., Alshehhi, A., Alzaabi, E., Albeloshi, A., Alfalasi, S., 2016. Air quality monitoring for sustainable systems via drone based technology. 2016 IEEE International Conference on Information and Automation for Sustainability (ICIAfS), pp. 1–5.

Wojnowski, W., Dymerski, T., G\kebicki, J., Namieśnik, J., 2019. Electronic noses in medical diagnostics. Curr. Med. Chem. 26, 197–215.

Wolf, C.A., Hardis, R.P., Woodrum, S.D., Galan, R.S., Wichelt, H.S., Metzger, M.C., Bezzo, N., Lewin, G.C., de Wekker, S.F.J., 2017. Wind data collection techniques on a multi-rotor platform. 2017 Systems and Information Engineering Design Symposium (SIEDS), pp. 32–37.

Wood, R., Nagpal, R., Wei, G.-Y., 2013. Flight of the Robobees. Sci. Am. 308, 60–65.

Xi, X., Johnson, M.S., Jeong, S., Fladeland, M., Pieri, D., Diaz, J.A., Bland, G.L., 2016. Constraining the sulfur dioxide degassing flux from Turrialba volcano, Costa Rica using unmanned aerial system measurements. J. Volcanol. Geotherm. Res. 325, 110–118.

Yang, J., Chen, B., Zhou, J., Lv, Z., 2015. A low-power and portable biomedical device for respiratory monitoring with a stable power source. Sensors 15, 19618–19632.

Yang, Y., Zheng, Z., Bian, K., Song, L., Han, Z., 2017. Real-time profiling of fine-grained air quality index distribution using UAV sensing. IEEE Internet Things J. 5, 186–198.

Yang, S., Talbot, R., Frish, M., Golston, L., Aubut, N., Zondlo, M., Gretencord, C., McSpiritt, J., 2018. Natural gas fugitive leak detection using an unmanned aerial vehicle: measurement system description and mass balance approach. Atmosphere (Basel) 9, 383.

Yuan, C., Zhang, Y., Liu, Z., 2015. A survey on technologies for automatic forest fire monitoring, detection, and fighting using unmanned aerial vehicles and remote sensing techniques. Can. J. For. Res. 45, 783–792.

Zhang, L., Zhang, D., 2014. Domain adaptation extreme learning machines for drift compensation in E-nose systems. IEEE Trans. Instrum. Meas. 64, 1790–1801.

Zhou, X., Aurell, J., Mitchell, W., Tabor, D., Gullett, B., 2017. A small, lightweight multipollutant sensor system for ground-mobile and aerial emission sampling from open area sources. Atmos. Environ. 154, 31–41.

Zhou, F., Pan, S., Chen, W., Ni, X., An, B., 2019. Monitoring of compliance with fuel sulfur content regulations through unmanned aerial vehicle (UAV) measurements of ship emissions. Atmos. Meas. Tech. 12.

Zuliani, C., Luque, J., Falco, C., Gardner, E., De Luca, A., Vincent, T., Tripathy, S., Ali, Z., Udrea, F., 2020. Flow compensated gas sensing array for improved performances in breathanalysis applications. IEEE Sensors Lett 4, 1–4.

**Glossary**

ABL: Atmospheric Boundary Layer
ANN: Artificial Neural Network
CEAS: Cavity Enhanced Absorption Spectroscopy
CFD: Computational Fluid Dynamics
CP-TDL: Closed-Path Tunable Diode Laser
CRDS: Cavity Ring-Down Spectroscopy
EC: Electrochemical Cell
E-nose: Electronic Nose
EPA: Environmental Protection Agency
FSC: Fuel Sulfur Content
FW: Fixed wing
GCM: Gas Concentration Mapping
GHG: Greenhouse Gas
GP: Gaussian Plume
GPS: Global Positioning System
GSL: Gas Source Localization
IED: Industrial Emissions Directive
IMO: International Maritime Organization
IR: Infrared
IT: Isotropic
LAS: Laser Absorption Spectroscopy
LDAR: Leak Detection and Repair
MMS: Miniature Mass Spectrometer

MOX: Metal Oxide
MTOW: Maximum Take-Off Weight
NDIR: Non-Dispersive Infrared
OA-ICOS: Off-Axis Integrated Cavity Output Spectroscopy
OGI: Optical Gas Imaging
OPLS: Open Path Laser Spectrometer
OP-TDL: Open Path Tunable Diode Laser
O&G: Oil and Gas
PID: Photo-Ionization Detector
PTV: Particle Tracking Velocimetry
RC: Radio Control
RPAS: Remotely Piloted Aircraft System
RPT: Reactive Plume Tracking
RW: Rotary Wing
SEM: Surface Emission Monitoring
sTDLAS: Standoff Tunable Diode Laser Absorption Spectroscopy
STILT: Stochastic Time-Inverted Lagrangian Transport
sUAS: Small Unmanned Aircraft System
SWL: Solid Waste Landfill
TDL: Tunable Diode Laser
TDLAS: Tunable Diode Laser Absorption Spectroscopy
TVOCs: Total Volatile Organic Compounds
UAS: Unmanned Aircraft System
UGV: Unmanned Ground Vehicle
UV: Ultraviolet
VLOS: Visual Line of Sight
VTOL: Vertical Take-Off and Landing
VOCs: Volatile Organic Compounds
WWTP: Wastewater Treatment Plant